Modulation of NF-κB activation in *T. annulata* infected cloned cell lines is associated with detection of parasite dependent IKK signalosomes and disruption of the actin cytoskeleton

Jacqueline Schmukli-Maurer[1], Jane Kinnaird[2], Sreerekha Pillai[2], Pascal Hermann[1], Sue McKellar[2], William Weir[2], Dirk Dobbelaere[1] and Brian Shiels[2]*

* For correspondence email b.shiels@vet.gla.ac.uk;

Tel. +44 (0) 141 330 5756;

Fax. +44 (0) 141 3305603

Running title: NF-κB activation is modulated in *Theileria* infected cells

Key words: *Theileria annulata*, NF-κB, IKK signalosomes, actin cytoskeleton

[1] Division of Molecular Pathobiology, Department of Clinical Research and VPH, Vetsuisse Faculty Bern, CH-3012 Bern, Switzerland

[2] Division of Veterinary Infection & Immunity, Institute of Comparative Medicine, Veterinary School, University of Glasgow, Bearsden Road, Glasgow, G61 1QH, Scotland, UK

Summary

Apicomplexan parasites within the genus *Theileria* have the ability to induce continuous proliferation and prevent apoptosis of the infected bovine leukocyte. Protection against apoptosis involves constitutive activation of the bovine transcription factor NF-κB in a parasite dependent manner. Activation of NF-κB is thought to involve recruitment of IKK signalosomes at the surface of the macroschizont stage of the parasite, and it has been postulated that additional host proteins with adaptor or scaffolding function may be involved in signalosome formation. In this study two clonal cell lines were identified that show marked differences in the level of activated NF-κB. Further characterisation of these lines demonstrated that elevated levels of activated NF-κB correlated with increased resistance to cell death and detection of parasite associated IKK signalosomes, supporting results of our previous studies. Evidence was also provided for the existence of host and parasite dependent NF-κB activation pathways that are influenced by the architecture of the actin cytoskeleton. Despite this influence, it appears that the primary event required for formation of the parasite dependent IKK signalosome is likely to be an interaction between a signalosome component and a parasite encoded surface ligand.

Introduction

Infection of bovine leukocytes by the parasites *Theileria annulata* and *Theileria parva* results in lymphoproliferative disorders that severely compromise livestock husbandry over much of Africa, Asia and regions of Southern Europe. Pathology of infection is linked to the ability of the parasite to modulate the phenotype of the host leukocyte it infects. Thus, following differentiation of the parasite into the macroschizont stage, infected host cells undergo a phase of uncontrolled proliferation (Irvin and Morrison, 1987). Moreover, the parasite overrides fail-safe checkpoints that protect against uncontrolled leukocyte proliferation by manipulating the pathways that regulate programmed cell death (Dessauge *et al.*, 2005; Heussler *et al.*, 1999). Other phenotypic changes to the infected host cell include a loss of cellular differentiation markers (Sager *et al.*, 1997) and altered expression profiles of host cell genes encoding cytokines, proteases, adhesion molecules and surface receptors (reviewed by (Ahmed *et al.*, 1999; Dobbelaere and Heussler, 1999)). Parasite-mediated manipulation of host cell phenotype contributes to the expansion, dissemination and virulence of the infected cell. In naïve *Bos taurus* breeds the outcome of infection is often death, due to respiratory failure caused by pulmonary oedema or widespread destruction and disorganisation of the lymphoid system (Irvin and Morrison, 1987).

Theileria-mediated mechanisms that orchestrate manipulation of the infected cell are not fully understood. It has been shown that parasite dependent activation of a number of leukocyte transcription factors plays a major role, as these factors can function as regulators of genes controlling proliferation, cell death or cytokine production. Such factors include AP-1 (Chaussepied *et al.*, 1998), ATF2 (Botteron and Dobbelaere, 1998),

STAT3, cMyc (Dessauge *et al.*, 2005) and NF-κB (Ivanov *et al.*, 1989). However, the points where the parasite hijacks the signal transduction pathways responsible for host cell transcription factor activation are largely unknown. The exception to this situation is the mechanism that brings about constitutive activation of NF-κB, as it has been demonstrated that activation is brought about by recruitment of the IKK signalosome complex close to the macroschizont surface (Heussler *et al.*, 2002). The resulting enforced oligomerisation of the IKK proteins is thought to be responsible for signalosome dependent kinase activity that leads to phosphorylation and constitutive degradation of the NF-κB inhibitors, IκB-α and IκB-β. Inhibitor degradation allows translocation of NF-κB to the leukocyte nucleus where it regulates its target genes.

The simplest model to account for parasite enforced signalosome formation is that a macroschizont membrane protein acts as a ligand for a critical component of the signalosome complex. However, such a direct association has not been demonstrated (Heussler *et al.*, 2002). This may be due to the requirement for additional host proteins with adaptor, scaffolding or activator properties (Dobbelaere and Rottenberg, 2003) and it has been proposed that components of the cytoskeleton could interact with the parasite surface and bring about patchy accumulation of IKK components at these sites (Dobbelaere and Kuenzi, 2004). In addition, it has been demonstrated that cytoskeletal structures act as an assembly platform to promote activation of IKK signalosomes in HTLV infected cells (Kfoury *et al.*, 2008).

A major control strategy against tropical theileriosis caused by *T. annulata* is the use of long-term cultures of parasite-infected cells as a live vaccine. Prolonged culture or cloning of infected cells results in major alterations to infected cell phenotype including a

loss of virulence, reduced expression of protease gene expression, altered cytokine profiles and significant reduction in the ability of the parasite to undergo differentiation to the merozoite stage of the life cycle, merogony (reviewed by (Hall *et al.*, 1999)). Such major changes to infected cell phenotype are likely to involve qualitative and or quantitative alterations to parasite dependent mechanisms that control host and parasite gene expression.

To identify factors and pathways responsible for variability between the phenotypes of different cell lines, an *in vitro* model system has been established. The system consists of parental (D7) and daughter (D7B12) cloned infected cell lines that display marked phenotypic differences, including the ability to undergo merogony (Shiels *et al.*, 1994). Subsequent study of the lines revealed significant differences in the levels of parasite-encoded DNA binding factors that are transported to the host nucleus and are postulated to operate as modulators of host cell gene expression and morphology (Shiels *et al.*, 2004; Swan *et al.*, 2001; Swan *et al.*, 2003). To assess the possibility that activated host cell transcription factors could also be associated with altered phenotypes displayed by *Theileria* infected cell lines, the present study compared the level of activated NF-κB in the D7 and D7B12 cloned cell lines. The results show that the level of NF-κB and parasite dependent IKK signalosomes are significantly different between these cell lines, and this difference was used to investigate the potential involvement of the host cell cytoskeleton in the formation of parasite dependent signalosome complexes.

Results

Levels of activated NF-κB are significantly elevated in the D7B12 infected cloned cell line relative to the parental D7 clone

Restriction fragment length polymorphism analysis indicated previously that parental D7 and daughter D7B12 cloned cell lines are represented by the same parasite genotype (Shiels *et al.*, 1994). To confirm that this was the case the two cell lines were re-typed using a set of polymorphic mini- and micro-satellite markers that have recently been developed for multi-locus genotyping of *Theileria* infected cell lines (Weir *et al.*, 2007). The analysis demonstrated that the PCR product generated for each marker was identical in size and that the two lines represent the same parasite genotype (Figure 1A). This result confirms that the D7 cell line represents a clonal line and that the D7B12 line is derived from the D7 clone. It should be noted though, that despite the apparent genotypic identity of the parasites in these two lines, it is extremely likely that alterations resulting in changes to parasite gene expression or protein function have occurred via point mutation or an epigenetic mechanism, as proposed previously (Shiels *et al.*, 1998).

To study whether host encoded nuclear transcription factors show altered levels between the D7 and D7B12 cloned cell lines, commercial antibodies specific for the p65 and p50 subunits of NF-κB and an anti-serum raised against the Octomer 2 factor (Oct-2) were used in an indirect immunofluorescence assay; previous studies had identified these factors in the nucleus of the D7 or D7B12 cell lines (Heussler *et al.*, 2002; Shiels *et al.*, 2004). As demonstrated by Figure 1B, the level of nuclear fluorescence detected by the NF-κB specific antibodies for D7B12 cells was clearly greater than that detected for D7 cells. This was manifest as elevated intensity of host nuclear fluorescence and an increase in the number of cells within a field that displayed host nuclear NF-κB staining. In contrast, there was no detectable difference in the level of nuclear staining detected with the Oct-2 antibody. Confirmation of elevated levels of NF-κB in the nucleus of D7B12

cells relative to D7 was obtained by immunoblotting extracts derived from cellular fractions representing the cytosol, membrane/organelle and nuclear fractions of both D7 and D7B12 cells. As shown in Figure 1C while the cytosol of D7 and D7B12 cells had comparable levels of the p50 sub-unit of NF-κB and its p105 precursor, the nuclear fraction of B12 contained significantly more p50 than the D7 extract. Both nuclear extracts showed significant depletion of the p105 precursor protein indicating enrichment of the nuclear fraction.

To test whether elevated detection of NF-κB proteins in the host nucleus of B12 cell lines is associated with elevated transcriptional activity, D7 and D7B12 cells were co-transfected with an NF-κB-dependent luciferase reporter plasmid and either the control pcDNA3 vector DNA or a pcDNA3-IκBαS32A construct that expresses a mutant IκBα protein that inhibits constitutive activation of NF-κB. The results showed that B12 cells displayed more than seven times greater reporter activity relative to D7 cells (Figure 1D). In addition, as the level of inhibition mediated by the inhibitor construct was comparable for both cell lines, it can be concluded that the difference in reporter activity reflects an increase in transcriptionally active NF-κB in the D7B12 cell line relative to D7.

Levels of parasite dependent IKK signalosome and phosphorylated IκBα are significantly elevated in D7B12 relative to D7 cells

Theileria dependent activation of NF-κB has been shown to involve aggregation of IKK signalosome complexes close to or at the surface of the macroschizont. Aggregation of the kinase complex results in phosphorylation of the NF-κB inhibitor, IκBα, which is then constitutively degraded (Heussler *et al.*, 2002; Palmer *et al.*, 1997). Based on this

model of activation it can be postulated that levels of parasite associated signalosome and phosphorylation of IκBα should be higher in the D7B12 line relative the D7 line. This postulation was tested by IFAT analysis using a monoclonal antibody specific to the modulating subunit IKKγ (NEMO), as a marker for the parasite associated signalosome complex. The results clearly showed that the number of signalosomes per parasite body and the number of cells per field with detectable signalosomes was significantly greater in the D7B12 cell line compared to D7 (Figure 2). However, considerable variability in the number of detectable signalosomes per parasite was observed, particularly between cells of the D7B12 cell line. As predicted from previous work (Heussler *et al.*, 2002) anti-IKKγ failed to produce a signal in uninfected BL20 cells, while the infected counterpart TBL20 possessed parasite-associated signalosomes (Figure 2). A monoclonal antibody (1C2) specific for a rhoptry protein of *T. annulata* (Shiels *et al.*, 1992) failed to generate signalosome like reactivity against D7B12 cells.

To assess the level of the phosphorylated form of IκBα (P-IκBα) immunoblotting using a phospho-specific antibody was performed. Extracts were generated from cells treated with a protease inhibitor (MG-132) to prevent constitutive degradation of P-IκBα (Devalaraja *et al.*, 1999). As shown by Figure 2 the level of P-IκBα was clearly stronger in the D7B12 extract relative to D7 and the uninfected control cell line BL20. Furthermore, in the absence of MG-132 treatment the steady state level of IκB was lower in the D7B12 extract relative to D7 and uninfected BL20 extracts. These results indicate higher levels of phosphorylation and degradation of IκBα in the D7B12 cell line.

D7B12 cells display increased resistance to cell death

NF-κB targets a wide range of genes that have the potential to significantly influence cellular phenotype. These targets include genes whose proteins control proliferation and apoptosis (Hinz *et al.*, 1999; LaCasse *et al.*, 1998). To determine whether D7B12 and D7 cells display similar or distinct growth profiles, viable cells were counted at 48, 96 and 120 hours. The results showed that at the day 2 time point the proliferation rate of D7B12 cultures was 24 % greater relative to D7, and that further culture to Day 4 elevated the difference to 33 % (see Figure 3A). In addition, the number of non-viable cells was over 2 fold greater in the D7 day 4 culture compared to D7. These results indicate that D7B12 cells proliferate slightly faster and show greater survival under conditions of stationary phase growth. To determine if this was due to an ability of these cells to prevent apoptosis caspase 3/7 activity was measured at Day 4 of culture. The results showed that caspase activity was significantly (3.4 fold) higher in the D7 culture relative to D7B12 (Figure 3B).

It is known that a viable parasite is required for constitutive activation of NF-κB and protection of the host cell from undergoing apoptosis (Heussler *et al.*, 1999; Heussler *et al.*, 2002; Ivanov *et al.*, 1989). Therefore, to kill the parasite, D7 and D7B12 cultures were treated with Bpq for 48 hours. The number of viable cells was counted and caspase activity measured to assess the level of apoptosis. The results showed that cell growth was reduced by 70 % in the D7 line compared to 43 % for D7B12 (Figure 3C). This difference in response to the drug was mirrored by the level of caspase activation, as Bpq treated D7 cells generated 4.3 fold more activity compared to no drug control cells, whereas Bpq treated D7B12 cells showed a smaller increase of 2.5 fold relative to the no drug control (Figure 3D). Efficacy of Bpq activity against parasite load was assessed by

immunoblotting infected cell extracts with an anti-serum raised against the Tasp macroschizont surface antigen (Schnittger *et al.*, 2002). The results indicate a significant reduction in the level of protein for both cell lines treated with Bpq, demonstrating the drug had the expected detrimental effect on the parasite of both cell lines (Figure 3E). Taken together the results indicate that D7B12 cells show increased viability and resistance to cell death compared to their D7 counterparts.

Activation of NF-κB in Theileria infected cells is associated with alteration of cellular morphology and manipulation of the actin cytoskeleton

To investigate potential mechanisms responsible for the variable level of parasite associated signalosomes detected between the D7B12 and D7 cell lines, analysis of the cytoskeleton of infected cells was undertaken because: interaction between the macroschizont surface and components of the host cell cytoskeleton has been described (Schneider *et al.*, 2007; Shaw, 1997); cytoskeletal structures could provide a scaffold for signalosome formation, and dynamic interaction between cytoskeleton and parasite surface may account for the variable and patchy accumulation of signalosomes on individual macroschizonts ((Heussler *et al.*, 2002) and this study, see Figure 2); previous work suggested that host cell shape is controlled by parasite infection (Shiels *et al.*, 2004) and standard monitoring of D7 and D7B12 cultures indicated differences in cell morphology (data not shown).

An initial comparison of *T. annulata* infected TBL20 with their uninfected BL20 counterpart confirmed that parasite infection results in significant alteration to the shape of the host leukocyte. As can be seen in Figure 4, BL20 cells have a uniform shape

whereas TBL20 cells display a more uneven elongated shape with numerous blebs and processes. In addition phalloidin staining revealed that the actin cytoskeleton appeared to consist of a denser network of actin filaments in the infected cells and that this network surrounded the host nucleus and macroschizont (Supplementary Data, Figure 1). Differences in morphology between D7 cells (low signalosomes) and D7B12 cells (high signalosomes) were confirmed by analysis of Giemsa stained cells, the latter showing a much more uniform round morphology with less membrane blebbing and pronounced processes relative to the D7 counterpart (Figure 4, panel 3 Vs panel 4). Differences were also seen in the pattern of actin fibres, D7B12 cells displaying a looser network of fibres surrounding the host nucleus and parasite relative to D7 cells (panel 7 Vs panel 8). Similar observations were obtained on analysis of the microtubule network, as in D7B12 cells the network appeared more evenly distributed across parasite and host nuclei (Figure 4, panels 9 - 12).

To test if host cell shape and signalosome detection are both dependent on a viable parasite, D7B12 cells were treated with Bpq for 48 hours and IFAT performed with anti-IKKγ. The results clearly show a loss of signalosome levels in Bpq treated cells and major changes to the shape of the host nuclei that, in general, became elongated and lobed and occasionally displayed a doughnut-like morphology (Figure 4, panels 13-16). Thus, there is a clear association between both gain and loss of parasite associated signalosomes and parasite dependent modulation of cell shape.

Disruption of the actin cytoskeleton in myeloid cells, the preferential cellular target for infection by *T. annulata,* has been shown to activate NF-κB (Bourgarel-Rey *et al.*, 2001; Kustermans *et al.*, 2005). To test whether actin filaments could provide a scaffold for

IKK signalosomes and influence NF-κB activation levels, D7 and D7B12 infected cell lines were treated with either cytochalasin D at 2.5 and 24 hours to dissociate actin filaments, or jasplakinolide at 24 hours to condense actin filaments, and NF-κB dependent luciferase reporter activity measured. The results showed that treatment with cytochalasin significantly increased the ratio of NF-κB dependent luciferase to TK renilla activity at 2.5 hours (Figure 5A) and that the ratio increased further following incubation of 24 hours in the drug (Figure 5B). In a similar manner to cytochalasin, jasplakinolide significantly elevated the relative level of NF-κB reporter activity following incubation in drug for 24 hours (Supplementary Data, Figure 2). To determine if elevated reporter activity was linked to elevated phosphorylation of the IκB inhibitor, immunoblots were performed and the detected P-IκBα normalised to actin levels following densitometry. The results (Figure 5C and D) showed that phosphorylated IκBα was elevated in both cell lines after incubation with cytochalasin D for 24 hours. Thus, manipulation of the actin cytoskeleton can result in activation of NF-κB via elevated phosphorylation of the IκBα inhibitor in *Theileria* infected cells. These results, however, do not provide confirmation that a particular arrangement of actin filaments provides a scaffold for parasite dependent signalosome activation.

Host and parasite associated NF-κB activation pathways can be manipulated by disruption of the cytoskeleton

Activation of NF-κB by incubation in cytochalasin D could occur by a host dependent, parasite dependent or combination of host and parasite dependent pathways. It has been demonstrated that treatment with geldanamycin disrupts critical HSP90 IKK interactions

to inhibit activation of NF-κB in mammalian cells (Broemer *et al.*, 2004), whereas *Theileria* dependent activation of NF-κB is largely resistant to the drug (Hermann and Dobbelaere, 2006). To test if the elevation in activity obtained following incubation with cytochalasin D was resistant to geldanamycin treatment, NF-κB reporter assays were carried out. As reported previously (Hermann and Dobbelaere, 2006), the results clearly show that geldanamycin only had a partial effect of inhibiting NF-κB reporter activity and did not remove detection of parasite dependent IKK signalosomes (Supplementary data, Figure 3A and B). Geldanamycin also had no inhibitory effect on the elevation of NF-κB reporter activity associated with cytochalasin D treatment of *Theileria* infected D7B12 cells (Supplementary data, Figure 3C).

NF-κB reporter assays were also conducted in uninfected BL20 cells and compared relative to the infected TBL20 line. The results showed that as expected the *Theileria* infected BL20 cells had significantly greater NF-κB reporter activity relative to uninfected BL20 (Supplementary data, Figure 3D). However, incubation with cytochalasin D showed a greater fold increase of NF-κB reporter activity for uninfected BL20 cells compared to the infected counterpart, although the absolute increase in activity was comparable. In addition, the elevation of NF-κB activity induced by cytochalasin D treatment of uninfected BL20 cells was slightly augmented by treatment with geldanamycin. It can be concluded that a host activation pathway that is independent of the HSP90 chaperone is induced by disruption of the actin cytoskeleton upon treatment with cytochalasin D.

To investigate the effect of cytochalasin D treatment at the level of the IKK signalosome, immunofluorescence analysis was conducted using the monoclonal antibody against

IKKγ. Two results were of note. Firstly in both D7 and D7B12 cells treated with cytochalasin D, a general increase of reactivity against IKKγ could be detected that was present in the cytoplasmic region of the cell and was not associated with the region occupied by the macroschizont (Figure 6 and Supplementary Data, Figure 4). Reactivity with a P-IκBα antibody also showed a similar increase in low-level cytoplasmic reactivity upon cytochalasin treatment (data not shown). Given that cytochalasin D treatment significantly increased the level of NF-κB activity in uninfected cells, we conclude that the general cytoplasmic IKK staining is likely to represent a host cell pathway involving low order signalosome formation that is induced upon disruption of the actin cytoskeleton.

Examination of the association between the signalosome and parasite was anlaysed by immunofluorescence and DAPI staining, and double labeling of IKKγ and Tasp. The results showed that cytochalasin D significantly altered the parasite associated IKK signalosome pattern, manifest as a reduction in the number of detected signalosome bodies per macroschizont (Table 1) and an increase in the detectable size of signalosomes (Figures 6 and 7). Thus, it appears that the parasite-associated signalosome can be qualitatively altered by treatment with cytochalasin D. In contrast, dissolution of microtubules by treatment with nocodazole had no significant effect on the detection of parasite signalosomes, and the general increase in the signalosomes size obtained by cytochalasin D treatment was not evident (see Figure 8).

To confirm that the actin cytoskeleton was disorganised, phalloidin staining of cytochalasin D treated cells was performed. As shown by Figure 7 treatment with cytochalasin cells resulted in a clear disruption, with re-ordering of the normal cellular

network of filaments into aggregates localised to a limited region of the host cell cytoplasm. These foci of actin filaments were found to be, in general, distinct from the location occupied by the DAPI stained macroschizont nuclei. Re-ordering of actin filaments into neo-formed aggregates following cytochalasin D treatment has been reported (Mortensen and Larsson, 2003; Schliwa, 1982). In contrast, the staining pattern obtained for the Tasp membrane protein showed a strong co-localisation with large signalosome foci in the presence of cytochalasin D (Figure 7, panel 4). Indeed, in some drug treated cells detected signalosomes appeared to be some distance from where the parasite nuclei were located, but these distant foci were always found to be associated with parasite membrane. Furthermore, parasites that had been released from cells during cytospin preparations also showed retention of IKK signalosomes, which appeared to be located at the parasite membrane (Supplementary Data, Figure 5).

To further investigate the association of IKK reactivity with components of the cytoskeleton the extraction procedure of Loeb and Hass (Loeb and Haas, 1994) was conducted. In this procedure progressive extraction of tubulin and actin networks is performed to leave intermediate filaments of the cytoskeleton. The extraction procedure showed no apparent reduction in the level of detection of parasite associated signalosomes in D7B12 cells but significantly reduced detection of actin filaments, the tubulin network, the Tasp macroschizont surface protein and the p65 subunit of NF-κB (Supplementary Data, Figure 6).

Discussion

Activation of NF-κB by *Theileria* parasites has been shown to be a critical event in the parasite dependent mechanism of host cell transformation. The results of this study demonstrate that two cloned cell lines (D7 and D7B12) represented by the same parasite genotype show markedly different levels of activated NF-κB. Thus, relative to its D7 parental clone, the D7B12 cloned cell line was shown to have elevated levels of activated NF-κB, grow faster and display increased resistance to conditions that induce cell death. Given previous work has shown that the function of activated NF-κB is to protect the parasite-infected cell from undergoing apoptosis, and may directly contribute to its proliferation (Dobbelaere and Rottenberg, 2003; Heussler *et al.*, 1999), it can be concluded that the superior ability of the D7B12 cell line to grow and survive in culture is linked to its elevated level of NF-κB activity. Indeed, treatment of both cell lines with the BMS-345541 inhibitor of NF-κB (Burke *et al.*, 2003) rapidly induced cell death (J.S. and D.D., data not shown).

The elevation in NF-κB activity displayed by the D7B12 cell line is likely to be related to a selection pressure for cells with a greater propensity to proliferate and survive under conditions of cell cloning by limiting dilution and may not, therefore, occur in natural populations of *T. annulata* infected leukocytes. Indeed the D7 cell line shows significantly lower levels of activated NF-κB and survives relatively well in culture, although we have not detected a total lack of NF-κB activity in any *Theileria* infected cell line to date. A number of studies, however, have indicated that phenotypic variability between *Theileria* infected cell lines cultured *in vitro*, including the profile of inflammatory cytokines they express, may be the rule rather than the exception (reviewed

by (Ahmed *et al.*, 1999; Dobbelaere and Heussler, 1999)). Such variability could involve altered levels of both host and parasite factors that operate to control leukocyte gene expression (Adamson *et al.*, 2000; Shiels *et al.*, 2004; Swan *et al.*, 2001; Swan *et al.*, 2003). This may point to a propensity of the parasite to vary the level of its control over infected cell phenotype, allowing adaptation to different cellular environments encountered within the host.

Previous work provided conclusive evidence for activation of NF-kB in *Theileria* infected cells via aggregation of the IKK signalosome complex at the macroschizont surface (Heussler *et al.*, 2002). In the present study, a strong correlation was obtained between elevated levels of parasite associated signalosomes, elevated levels of phosphorylated IκBα and activation of NF-κB. In addition, treatment with buparvaquone to kill the parasite resulted in a loss of detectable IKK foci, and it is known that parasite death is coincident with a reversal of constitutive NF-κB activation (Heussler *et al.*, 2002; Ivanov *et al.*, 1989). Thus, while contribution of additional pathways such as the TNFα autocrine loop proposed by (Guergnon *et al.*, 2003) have not been excluded, the results of this study strongly support the previous model of proximity-induced IKK activation (Heussler *et al.*, 2002). We conclude that interaction between parasite and host cell components in the D7B12 cell line provides a platform that allows formation of the signalosome complex with greater efficiency than its D7 counterpart.

A working model proposed to account for formation of *Theileria* associated IKK signalosomes includes postulation of a parasite surface ligand that binds a component of the IKK complex and additional host adaptor proteins that may be components of the cytoskeleton. Unfortunately, this model could not be fully tested by the present study

since a direct association between a parasite protein and IKK has not been demonstrated (Heussler *et al.*, 2002). Evidence that the cytoskeleton could influence parasite dependent IKK signalosomes was provided by observation that the cytoskeleton of D7 and D7B12 cells is markedly different. In addition, comparison of BL20 cells with TBL20 cells and the detection of shape changes upon buparvaquone treatment indicate that the parasite actively controls the cytoskeleton of the bovine leukocyte. How the parasite accomplishes this requires further study. Nevertheless, it may be of relevance that parasite encoded (TashAT family) proteins which translocate to the host nucleus have been shown to significantly modulate the profile of cytoskeletal proteins of transfected cells (Oura *et al.*, 2006; Shiels *et al.*, 2004). Since levels of TashAT family proteins detected in the nuclei of D7 and D7B12 cells vary significantly (Swan *et al.*, 2001; Swan *et al.*, 2003), it is possible that they contribute to the differences in the cytoskeletal architecture displayed by these cell lines.

To test if the cytoskeleton was involved in providing a platform for parasite dependent signalosome formation, microtubule and microfilament structures were disrupted by drug treatment. The results were complicated, however, by clear evidence for a host NF-κB activation pathway that may operate via lower order signalosomes detected in the host cell cytoplasm. Recent work in myeloid cells has led to a model whereby cytochalasin D disruption of actin filaments located at membrane ruffles is proposed to release the Nod2 protein which then promotes IKK signalosome activation by binding the RICK/RIP kinase (Legrand-Poels *et al.*, 2007). This pathway is a candidate mechanism for elevation of host-dependent signalosome activity in *Theileria annulata* infected cells. However, further work is required to establish that this is the case, particularly since the region of

the cytoplasm of cytochalasin treated cells that reacted with anti-IKKγ co-localised with neo-formed aggregates of actin filaments (data not shown).

The identification of the host activation pathway confounded conclusion that microfilament disruption can modulate activation of NF-κB via parasite dependent IKK signalosome activity. A qualitative effect of parasite-associated signalosomes was clearly discernable however, in that signalosomes located to the parasite became larger in size and fewer in number per parasite body. Despite this qualitative effect evidence that the cytoskeleton directly provides a template for parasite associated signalosome aggregation was not obtained. Thus, upon cytochalasin treatment displaced bundles of actin fibres detected by phalloidin did not show co-localisation with the large parasite associated IKK complexes. In contrast, the association between parasite dependent signalosomes and the parasite membrane was demonstrated to be strong, as signalosomes displaced from the location of parasite nuclei by drug treatment were found to be associated with strands of parasite membrane pulled from the main body of the parasite (see Figure 7).

Based on these results it can be concluded that a strong primary interaction between a parasite ligand and IKK components occurs. The formation of parasite associated IKK signalosomes, however, appears to be malleable and is likely to be influenced by the architecture of the cytoskeleton. Enforced re-ordering/clustering of a complex involving a parasite membrane protein(s), signalosome components and the cytoskeleton could account for the change in signalosome structure brought about by disorganisation of the actin cytoskeleton. This type of event has been demonstrated in fibroblast cells, where disruption of dynamic interactions between proteins located in the nuclear envelope that

are linked to the cytoskeletal network result in the formation of enlarged globular structures at displaced locations (Nery *et al.*, 2008).

In conclusion, this study has provided evidence that cell lines infected with *T. annulata* can show significant differences in their ability to activate host NF-κB via IKK signalosomes associated with the macroschizont, strongly supporting this activation pathway. However, definitive identification of *Theileria* or host proteins that act as a platform for the formation of parasite dependent IKK complex remains elusive. Our results support involvement of a parasite membrane protein that acts as a ligand and is expressed at elevated levels or provides enhanced IKK binding in D7B12 cells. A possible candidate is a recently identified macroschizont membrane protein of *T. parva* that has been shown to bind actin and activate NF-κB when transfected into mammalian cells (Hayashida and Sugimoto, personal communication). Further candidates may be obtained by exploiting the quantitative difference in parasite dependent signalosomes displayed by the D7 and D7B12 cell lines. Work to identify genes encoding macroschizont membrane proteins that are elevated in the D7B12 cell line is in progress.

Experimental procedures

Cell lines, cell culture and drug treatment

The uninfected lymphosarcoma cell line and its *T. annulata* infected counterpart were derived and cultured, as described in (Swan *et al.*, 2003). The infected cloned cell lines obtained by limiting dilution were maintained in culture by passage every two to three days (Shiels *et al.*, 1994). To characterise, in more detail, the parasite genotype represented by each clone, a panel of mini- and micro-satellite DNA markers developed

for genotyping of *T. annulata* isolates was used. The markers and methodology used for typing are as described by (Weir *et al.*, 2007).

In a range of experiments cultures were treated with the following drugs: buparvaquone (Bpq, Heumann PCS GmbH); cytochalasin-D (Cyt-D, Sigma); geldanamycin (GA, Invivogen); jasplakinolide (Jsp, Calbiochem); MG-132 (Sigma) and Z-VAD-FMK (Sigma). The optimal dose of drug was derived from titration experiments (Cyt-D and Jsp) or, a drug concentration based on an established protocol was employed for Bpq, Z-VAD-FMK (Oura *et al.*, 2006) and geldanamycin (Hermann and Dobbelaere, 2006). Details of drug concentrations and length of incubation are given in legends to Figures. The BMS-345541 inhibitor of IκB kinase (a kind gift from Dr James R. Burke, Bristol-Myres Squibb, New York, NY) was used at a concentration of 25 μM.

Cell viability counts and caspase assays

To assess the potential to survive under stationary phase growth conditions, 4 replicate cultures of D7 and D7B12 seeded with 1 x 10^5 cells ml^{-1} were incubated for four days at 37 ºC, under normal culture conditions. The number of viable and non-viable cells for each culture was determined (essentially as outlined by (Shiels *et al.*, 1992)) by a 1:1 dilution of cell suspension with 0.4 % trypan blue (Gibco) and counting cells that excluded or took up stain using a haemocytometer; differences between means were tested by standard statistical formulae (Harper, 1971), using *t* distribution analysis, with the difference between means concluded as being significant at the 95 % level of confidence ($p < 0.05$). Estimation of viable cell counts for cultures incubated in Bpq

were performed as described above, except cultures were incubated in the presence or absence of 50 ng ml^{-1} of drug for 48 hours.

To measure caspase-3 and caspase-7 activities the Caspase-Glo 3/7 assay (Promega) was utilised. Assays were performed for 4 replicate cultures per condition, according to the manufacturer's protocol. Briefly, cell cultures were diluted in culture medium to give 2 x 10^4 cells 100 μl^{-1}, and 50 µl of cell suspension mixed with 50 µl of Caspase-Glo 3/7 reagent and incubated for one hour at room temperature. Luminescence for each sample was then measured using a TD-20/20 luminometer (Turner Designs). Mean values, standard error and bar charts were generated using the Microsoft Excel: mac software package. Statistical analysis of the difference between mean values was carried out as described above.

Giemsa staining and Immunofluorescence analysis

Morphological examination of Giemsa stained cytospin cell preparations was conducted as previously described (Shiels *et al.*, 1992). Indirect immunofluorescence analysis of uninfected, infected and drug treated cells was performed essentially as described by (Shiels *et al.*, 1992; Shiels *et al.*, 2004), but with the following modifications. For detection of the p50 and p65 subunits of NF-κB and the Oct-2 transcription factor, cells deposited on slides using a cytospin were fixed immediately in ice-cold 4 % paraformaldehyde-phosphate buffered-saline (PBS), pH 7.4, for 30 minutes on ice. Slides were then washed X3 in PBS, incubated for 5 minutes in methanol pre-chilled to -20 ºC and washed X3 with PBS. For detection of actin filaments, IKKγ, Tasp and tubulin, cells on cytospin slides were air dried for 5 minutes, incubated in 4 % paraformaldehyde-PBS

at 4 ºC for 30 minutes, washed X3 with PBS, incubated in 0.2 % Triton-X-100 for 10 minutes at RT and washed X3 with PBS. Fixed cells were then incubated with the following primary antibodies/reagent: anti-IKKγ/NEMO (BD Biosciences 611306), used at a dilution of 1/50; anti-NF-κB p50 (E10) (Santa Cruz sc-8414), used at 1/500; anti-NF-κB p65 (C-20) (sc-372), used at 1/50; anti-Oct-2 (C-20) (Santa Cruz sc-233) used at 1/400; anti-Tasp (a kind gift from Jabbar Ahmed, Borstel), used at 1/200,000; anti-rhoptry monoclonal 1C2, neat hybridoma culture supernatant; Monoclonal anti-Tyrosine-Tubulin (Sigma T 9028), used at 1/500 and Alexa Fluor 488 phalloidin (Invitrogen A-12379) at 165 nM. Secondary antibodies used were Alexa Fluor 488 goat anti-rabbit (Invitrogen A-11034) or goat anti-mouse IgG (Invitrogen A-11029), both used at a dilution of 1/200. Images were acquired using an Olympus BX60 microscope, SPOT camera and SPOT image software (Diagnostic Instruments, Inc.). Matched exposures were used for immunofluorescence images of D7 Vs D7B12 cells.

Cell fractionation, immunoblotting and densitometry

Cell fractionation was performed on slides for immunofluorescence and in solution for immunoblotting. For immunofluorescence cells deposited on cytospin slides were sequentially extracted by the method of (Loeb and Haas, 1994). Briefly, to extract microtubules but retain actin and intermediate filaments, cytospin slides were incubated in 100 mM PIPES (pH 6.9), 0.5 mM $MgCl_2$, 0.1 mM EDTA (stabilisation buffer) with 0.5 % Triton X-100 for 30 minutes at 37 ºC. To extract actin filaments, the initial extraction in stabilisation buffer/Triton X-100 was followed by incubation with 0.3 M KI

for 3 hours at 4 ºC. Extracted cells were then fixed with paraformaldehyde and immunofluorescence analysis performed as described above.

For immunoblotting cell fractionation was performed using the ProteoExtract Sub-cellular Proteome Extraction Kit (S-PEK, Merckbiosciences/Calbiochem). The four sub-cellular fractions were obtained from 5 x 10^6 D7 or D7B12 cells by following the detailed protocol of the supplier. Extracts were concentrated using the ProteoExtract Protein Precipitation Kit (Merckbiosciences/Calbiochem) following the supplier's protocol. Estimate of protein per sample was obtained by SDS-PAGE and staining gels with Coomasie brilliant blue, as previously described (Shiels *et al.*, 2004). Equivalent amounts of protein per sample were loaded onto SDS-PAGE gels and immunoblotting and blot development performed as outlined (Shiels *et al.*, 1994; Swan *et al.*, 2001). The anti-NF-κB p50 antibody was used at a dilution of 1/1000.

For detection of phosphorylated IκBα (P-IκBα) and IκBα, 2 x 10^6 D7 or D7B12 cells were pretreated with the proteosome inhibitor MG132 (Sigma, C2211) at 4 μg ml^{-1} for 3 hours at 37 ºC. Cells were harvested, extracted in SDS-sample buffer and immunoblotted as described previously (Shiels *et al.*, 1994). The blotted samples were probed using the protocol of (Hermann and Dobbelaere, 2006). Primary antibodies were: anti-Phospho-IκB-α (Ser32) (Cell Signaling 9241) used at 1/1000; anti-IκBα (Santa Cruz sc-371) used at a dilution of 1/500, anti-tubulin (as above), used at 1/1000 and anti-actin (Santa Cruz, SC-1616) used at 1:500. Secondary antibodies were: horseradish peroxidase-conjugated goat anti-rabbit antibody (Cell Signaling, 7074), horseradish peroxidase-conjugated rabbit anti-mouse IgG (Dako P0260) and horseradish peroxidase-conjugated donkey anti-goat antibody (Santa Cruz, SC-2020) all diluted 1/2000. Blots

were developed using enhanced chemiluminescence reaction (ECL) using the manufacturers (Amersham Biosciences) protocol and SuperRX Fuji film. Densitometry was performed with Fujifilm Luminescent image analyzer (LAS-3000), using Aida software (version 4.10). Values given for P-IκBα were normalised with those obtained for the actin band of each cellular condition.

NF-κB reporter assay

Transient transfections and assay of luciferase activity were performed using the NF-κB_3-luciferase plasmid, Renilla luciferase plasmid and pcDNA3-IκBα^{S32A} or pcDNA3 plasmid, as detailed by (Heussler *et al.*, 2001). For assessment of drug treatment, 4 x 10^6 cells were re-suspended in 300 µl of RPMI-1640, 2 % foetal calf serum. 1.5 µg of NF-kB_3 and 0.25 µg of Renilla reporter plasmid were added and the cells electroporated using a BIO RAD gene pulser set at 220 V, 950 µF. Electroporated cells were added to 1.5 ml pre-warmed culture medium and cultured overnight. Drugs or an equal volume of DMSO were then added and cells cultured for 2.5 or 24 hours. Cells were then harvested by microfugation for two minutes (X960 rcf) and assays performed using the dual luciferase assay kit (Promega) and a TD-20/20 luminometer. NF-κB activity was expressed as the ratio of firefly luciferase activity over Renilla luciferase activity.

Reporter assays assessing luciferase activity in the presence or absence of the dominant negative pcDNA3-IκBα^{S32A} inhibitor plasmid were conducted, as described by (Hermann and Dobbelaere, 2006). Results were expressed as a percentage value relative to D7 cells transfected with both reporter constructs and the control pcDNA3 vector (set at 100 %).

Each electroporation and luciferase assay was performed in triplicate or quadruplicate: means, standard errors and bar charts were generated using the Microsoft Excel: mac software package.

Table 1. Number of schizonts with more than five or less than four signalosomes in a D7B12 culture treated for 2.5 hours with cytochalasin-D (25 µM) or jasplakinolide (0.5 µM) vs no drug control

	More than 5 signalosomes / schizont	Less than 4 signalosomes / schizont
No drug	35	67
Cytochalasin-D	12	99
Jasplakinolide	11	93

Figure legends

Figure 1. *Theileria* infected cell lines D7 and D7B12 show significant differences in activation level of NF-κB. A. Profile obtained with a panel of satellite markers (TS5-TS31), the size of the PCR product amplified for each marker is in base pairs (bp). B. Immunofluorescence analysis of NF-κB levels in D7 and D7B12 cell lines: panels 1 and 2, anti-p50 against D7 and D7B12 cells, respectively; panels 3 and 4, anti-p65 against D7 and D7B12 cells, respectively; panels 5 and 6, anti-Oct-2 against D7 and D7B12 cells, respectively. Bar = 25 μm. C. Immunoblot of extracts derived from cytoplasmic (cyto) or nuclear (nuc) SPEK fractions of D7 and D7B12 cells probed with antibody specific for the p50 subunit of NF-κB. The p105 precursor and p50 proteins are denoted. D. Relative luciferase activity of an NF-kB reporter construct transfected into D7, D7B12 and uninfected BL20 cells in the absence or presence of the IκBα^{S32A} inhibitor plasmid (S32A); results are expressed as % normalised luciferase activity relative to D7 cells transfected in the absence of inhibitor plasmid, set at 100 %.

Figure 2. D7B12 cells display elevated levels of parasite associated IKK signalosomes and P-IκBα. A. Immunofluorescence analysis of IKK signalosomes using a mouse monoclonal anti-IKKγ: panels 1 and 2, IKK signalosomes (green) and IKK signalosomes merged with DAPI stained nuclei (blue) of D7 cells, respectively; panels 3 and 4, IKK signalosomes and IKK signalosomes merged with DAPI stained nuclei of D7B12 cells; panels 5 and 6, IKK signalosomes and IKK signalosomes merged with DAPI stained nuclei of TBL20 cells, respectively; panel 7, uninfected BL20 cells reacted with

anti-IKKγ; panel 8, D7B12 cells reacted with control mouse monoclonal antibody 1C2. Bar = 22 μm, ps denotes parasite associated signalosomes. B. Immunoblot analysis of P-IκBα levels. Protein extracts were derived from D7, D7B12 and BL20 cell cultures, incubated in the presence of absence of the protease inhibitor MG-132, blots probed with anti-P-IκBα (upper panel), anti-IκBα (lower panel) and anti-tubulin control.

Figure 3. D7B12 cells display elevated resistance to cell death. A. Number of viable (V) and nonviable (NV) cells after culture for four days of D7 and D7B12 cells to stationary phase, * and + denote a significant difference between the means of viable and non-viable cell counts of four replicate D7 and D7B12 cultures, respectively ($p < 0.05$). B. Caspase 3/7 activity assayed for D7 and D7B12 stationary phase cultures, * denotes a significant difference between the means of four replicate D7 and D7B12 cultures ($p < 0.01$). C. Number of viable cells after culture of D7 and D7B12 in presence of 50 ng ml^{-1} buparvaquone (Bpq) or no drug (ND) for two days, * denotes a significant difference between the means of four replicate D7 and D7B12 Bpq treated cultures ($p < 0.01$). D. Caspase 3/7 activity for D7 and D7B12 cells cultured in Bpq or ND, * denotes a significant difference between the means of four replicate D7 and D7B12 cultures treated with Bpq ($p < 0.05$). E. Immunoblot analysis of extracts derived from D7, D7B12 and BL20 cell cultures following Bpq treatment for 0, 1, 2 or 3 days. The blot was probed with anti-Tasp and anti-tubulin specific antibodies.

Figure 4. *Theileria* infected and uninfected BL20 cells display differences in morphology and cytoskeletal architecture. Panels 1-4, BL20, TBL20, D7 and D7B12 cells,

respectively, stained with Giemsa. Bar = 29 μm. Panels 5-8, BL20, TBL20, D7 and D7B12 cells, respectively, reacted with Alexa Fluor 488 phalloidin (green) for detection of actin filaments, following extraction of microtubules with 0.5 % Triton X-100. Panels 9 and 10, D7 cells and D7B12 cells, respectively, reacted with a monoclonal antibody specific for tubulin. Panels 11 and 12: merge of DAPI stained nuclei (blue) and anti-tubulin staining (green) of D7 and D7B12 cells, respectively. Panels 13 and 14, IKK signalosomes (green), detected by anti-IKKγ, of D7B12 cells incubated in no drug (ND) or 50 ng ml^{-1} Bpq for two days. Panels 14 and 16, DAPI stained nuclei of D7B12 cells incubated in no drug (ND) or 50 ng ml^{-1} Bpq for two days. Bar = 19 μm, ps denotes parasite associated signalosomes, p denotes parasite nuclei.

Figure 5. Activated NF-κB and P-IκBα levels are elevated by disruption of the actin cytoskeleton. A. Ratio of Firefly/Renilla luciferase activity assayed for D7 and D7B12 cultures incubated with no drug (ND) or 25 μM cytochalasin D (Cyt-D) for 2.5 hours, * denotes a significant a difference between means of four replicate D7 and D7B12 ND cultures ($p < 0.05$). B. Ratio of Firefly/Renilla luciferase activity assayed for D7 and D7B12 cultures incubated with no drug (ND) or 25 μM cytochalasin D (Cyt-D) for 24 hours, + denotes a significant a difference between means of four replicate D7 and D7B12 ND cultures ($p < 0.05$), * denotes a significant difference between Cyt-D treated and ND cultures ($p < 0.01$). C. Immunoblot of cell extracts of D7 and D7B12 cultures treated with no drug (ND) or 25 μM cytochalasin D for 24 hours probed with anti-P-IκBα or anti-actin antibodies. D. Densitometry values of P-IκBα bands detected by immunoblotting after treatment of D7 and D7B12 with (Cyt-D) or without (ND)

cytochalasin D. Values are given as relative band intensity, following normalisation based on the signal detected for actin.

Figure 6. Cytochalasin D modulates immunofluorescence pattern of parasite and host associated IKKγ. Panels 1-3: IKKγ pattern (green) on D7B12 cells treated with 25 mM cytochalasin D (Cyt-D) for 24 hours, DAPI stained nuclei and merge of IKK and DAPI patterns, respectively; ps denotes parasite associated signalosomes and h denotes host cytoplasm associated staining. Panels 4-6: IKKγ pattern (green) on D7B12 cells treated with no drug (ND) for 24 hours, DAPI stained nuclei and merge of IKK and DAPI patterns, respectively; ps denotes parasite associated signalosomes. Panels 7-9: D7B12 cells treated with 25 µM cytochalasin D (Cyt-D) for 24 hours reacted with control monoclonal antibody 1C2, DAPI stained nuclei and merge of 1C2 and DAPI patterns, respectively. Bar = 19 µm.

Figure 7. Enlarged IKK signalosomes associate strongly with parasite membrane. Panel 1: merged image of D7B12 cells treated with 25 mM cytochalasin D (Cyt-D) for 2.5 hours reacted with DAPI (blue) and Alexa Fluor 488 phalloidin (green); p denotes parasite nuclei; a denotes foci of actin filaments. Panel 2: merged image of no drug treated (ND) D7B12 cells reacted with DAPI and IKKγ (red); ps, denotes parasite associated signalosomes. Panel 3: merged image of cytochalasin treated (Cyt-D) D7B12 cells reacted with DAPI and IKKγ (red); ps, denotes enlarged parasite associated signalosomes. Panel 4: merged image of cytochalasin treated (Cyt-D) D7B12 cells

reacted with anti-Tasp (green) and IKKγ (red); ps, denotes enlarged parasite associated signalosomes. Bar = 23 μm.

Figure 8. Detection of IKK associated signalosomes is resistant to de-polymerisation of microtubules by nocodazole. Panel 1: merge of images of DAPI stained nuclei (blue) and IKK signalosomes detected by anti-IKKγ (green) in D7B12 cells cultured with no drug (ND). Panel 2: merge of images of DAPI stained nuclei and IKK signalosomes in D7B12 cells cultured with 10 μM nocodazole for 20 hours (Noc). Panel 3: merge of images of DAPI stained nuclei (blue) and microtubules, detected by anti-tubulin (green), in D7B12 cells cultured with no drug. Panel 4: merge of images of DAPI stained nuclei (blue) and anti-tubulin staining in D7B12 cells cultured with nocodazole. Bar = 17 μm.

Supplementary Data - Figure legends

Figure 1. Actin network surrounds parasite and host nucleus. Merged images of DAPI stained nuclei (blue) and actin cytoskeleton detected by Alexa Fluor 488 phalloidin (green). Panel 1: BL20 cells; Panel 2: TBL20 cells; Panel 3: D7 cells; Panel 4: D7B12 cells. Microtubules were extracted from cells prior to fixation and staining. Bar = 22 μm, p denotes parasite nuclei.

Figure 2. Ratio of Firefly/Renilla luciferase activity assayed for D7 and D7B12 cultures incubated with no drug (ND) or 500 nM jasplakinolide for 24 hours, * denotes a

significant a difference between means of four replicate D7 and D7B12 ND cultures ($p < 0.05$).

Figure 3. Elevated activation of NF-κB is resistant to geldanamycin. A. Ratio of Firefly/Renilla luciferase activity assayed for D7B12 cultures incubated with no drug (ND) or 500 nM geldanamycin (GA) for 24 hours. B. Immunofluorescence analysis of IKK signalosomes using anti-IKKγ: panels 1 and 2, IKK signalosomes (green) of D7B12 cells incubated with no drug (ND) or 500 nM geldanamycin (GA) for 24 hours. Bar = 21 μm. C. Ratio of Firefly/Renilla luciferase activity assayed for D7B12 cultures incubated with no drug (ND), 25 μM cytochalasin D (Cyt-D) or 25 μM cytochalasin D plus 500 nM geldanamycin (GA) for 24 hours. D. Ratio of Firefly/Renilla luciferase activity assayed for BL20 and TBL20 cultures incubated with no drug (ND), 25 μM cytochalasin D (Cyt-D) or 25 μM cytochalasin D plus 500 nM geldanamycin (GA) for 24 hours; * denotes a significant difference between the means of hours replicate BL20 (ND) and BL20 (Cyt-D) cultures ($p < 0.01$), + denotes a significant difference between the means of four replicate BL20 (ND) and TBL20 (ND) cultures ($p < 0.01$).

Figure 4. Cytochalasin D modulates immunofluorescence pattern of parasite and host associated IKKγ in D7 cells. Panels 1-3: IKKγ pattern (green) on D7 cells treated with 25 mM cytochalasin D (Cyt-D) for 24 hours, DAPI stained nuclei and merge of IKK and DAPI patterns, respectively; ps denotes parasite associated signalosomes and h denotes host cytoplasm associated staining. Panels 4-6: IKKγ pattern (green) on D7 cells treated with no drug (ND) for 24 hours, DAPI stained nuclei and merge of IKK and DAPI

patterns, respectively; ps denotes parasite associated signalosomes. Panels 7-9: D7 cells treated with 25 μM cytochalasin D (Cyt-D) for 24 hours reacted with control monoclonal antibody 1C2, DAPI stained nuclei and merge of 1C2 and DAPI patterns, respectively. Bar = 22 μm.

Figure 5. Parasite dependent IKK signalosomes can be detected on isolated parasites and associate with staining of the macroschizont membrane by anti-Tasp. Panel 1: merge of immunofluorescence staining with anti-IKKγ (red) and DAPI (blue) of liberated schizonts from cytospin of D7B12 cells. Panel 2: merge of immunofluorescence staining with anti-Tasp antibody (green) and anti-IKKγ (red) of liberated schizonts. Bar = 8 μm, ps denotes parasite associated signalosomes.

Figure 6. Parasite associated signalosomes can be detected following extraction of microtubules and actin filaments. Panel 1: merge of DAPI stained nuclei and IKKγ staining (green) of control D7B12 cells. Panel 2: merge of DAPI stained nuclei and IKKγ staining (green) of D7B12 cells following sequential extraction of microtubules and actin filaments. Panels 3 and 4: detection of actin filaments by Alexa Fluor 488 phalloidin (green) of control and extracted cells, respectively. Panels 5 and 6: immunofluorescence detection of tubulin (green) of control and extracted cells, respectively. Panels 7 and 8: immunofluorescence detection of parasite membrane protein Tasp (green) of control and extracted cells, respectively. Panels 9 and 10: immunofluorescence detection of nuclear NF-κB, by anti-p65, of control and extracted cells, respectively. Bar = 25 μm.

Acknowledgements

This work was supported by the Wellcome Trust (075820), the Swiss National Science Foundation (Nr 3100A0-116653) and the Integrated Consortium on Ticks and Tick-borne Diseases ICTTD (Nr 510561).

References

Adamson, R., Logan, M., Kinnaird, J., Langsley, G., and Hall, R. (2000) Loss of matrix metalloproteinase 9 activity in *Theileria annulata*-attenuated cells is at the transcriptional level and is associated with differentially expressed AP-1 species. *Mol Biochem Parasitol* **106:** 51-61.

Ahmed, J.S., Schnittger, L., and Mehlhorn, H. (1999) Review: *Theileria* schizonts induce fundamental alterations in their host cells. *Parasitol Res* **85:** 527-538.

Botteron, C. and Dobbelaere, D. (1998) AP-1 and ATF-2 are constitutively activated via the JNK pathway in *Theileria parva*-transformed T-cells. *Biochem Biophys Res Commun* **246:** 418-421.

Bourgarel-Rey, V., Vallee, S., Rimet, O., Champion, S., Braguer, D., Desobry, A., Briand, C., and Barra, Y. (2001) Involvement of nuclear factor kappaB in c-Myc induction by tubulin polymerization inhibitors. *Mol Pharmacol* **59:** 1165-1170.

Broemer, M., Krappmann, D., and Scheidereit, C. (2004) Requirement of Hsp90 activity for IkappaB kinase (IKK) biosynthesis and for constitutive and inducible IKK and NF-kappaB activation. *Oncogene* **23:** 5378-5386.

Burke, J.R., Pattoli, M.A., Gregor, K.R., Brassil, P.J., MacMaster, J.F., McIntyre, K.W., Yang, X., Iotzova, V.S., Clarke, W., Strnad, J., Qiu, Y., and Zusi, F.C. (2003) BMS-345541 is a highly selective inhibitor of I kappa B kinase that binds at an allosteric site of the enzyme and blocks NF-kappa B-dependent transcription in mice. *J Biol Chem* **278:** 1450-1456.

Chaussepied, M., Lallemand, D., Moreau, M.F., Adamson, R., Hall, R., and Langsley, G. (1998) Upregulation of Jun and Fos family members and permanent JNK activity lead to constitutive AP-1 activation in *Theileria*-transformed leukocytes. *Mol Biochem Parasitol* **94:** 215-226.

Dessauge, F., Hilaly, S., Baumgartner, M., Blumen, B., Werling, D., and Langsley, G. (2005) c-Myc activation by *Theileria* parasites promotes survival of infected B-lymphocytes. *Oncogene* **24:** 1075-1083.

Devalaraja, M.N., Wang, D.Z., Ballard, D.W., and Richmond, A. (1999) Elevated constitutive IkappaB kinase activity and IkappaB-alpha phosphorylation in Hs294T melanoma cells lead to increased basal MGSA/GRO-alpha transcription. *Cancer Res* **59:** 1372-1377.

Dobbelaere, D. and Heussler, V. (1999) Transformation of leukocytes by *Theileria parva* and *T. annulata*. *Annu Rev Microbiol* **53:** 1-42.

Dobbelaere, D.A. and Kuenzi, P. (2004) The strategies of the *Theileria* parasite: a new twist in host-pathogen interactions. *Curr Opin Immunol* **16:** 524-530.

Dobbelaere, D.A. and Rottenberg, S. (2003) *Theileria*-induced leukocyte transformation. *Curr Opin Microbiol* **6:** 377-382.

Guergnon, J., Chaussepied, M., Sopp, P., Lizundia, R., Moreau, M.F., Blumen, B., Werling, D., Howard, C.J., and Langsley, G. (2003) A tumour necrosis factor alpha autocrine loop contributes to proliferation and nuclear factor-kappaB activation of *Theileria parva*-transformed B cells. *Cell Microbiol* **5:** 709-716.

Hall, R., Ilhan, T., Kirvar, E., Wilkie, G., Preston, P.M., Darghouth, M., Somerville, R., and Adamson, R. (1999) Mechanism(s) of attenuation of *Theileria annulata* vaccine cell lines. *Trop Med Int Health* **4:** A78-A84.

Harper,W.M. (1971) *Statistics*. London: Macdonald and Evans.

Hermann, P. and Dobbelaere, D.A. (2006) *Theileria*-induced constitutive IKK activation is independent of functional Hsp90. *FEBS Lett* **580:** 5023-5028.

Heussler, V.T., Kuenzi, P., Fraga, F., Schwab, R.A., Hemmings, B.A., and Dobbelaere, D.A. (2001) The Akt/PKB pathway is constitutively activated in *Theileria*-transformed leucocytes, but does not directly control constitutive NF-kappaB activation. *Cell Microbiol* **3:** 537-550.

Heussler, V.T., Machado, J., Jr., Fernandez, P.C., Botteron, C., Chen, C.G., Pearse, M.J., and Dobbelaere, D.A. (1999) The intracellular parasite *Theileria parva* protects infected T cells from apoptosis. *Proc Natl Acad Sci U S A* **96:** 7312-7317.

Heussler, V.T., Rottenberg, S., Schwab, R., Kuenzi, P., Fernandez, P.C., McKellar, S., Shiels, B., Chen, Z.J., Orth, K., Wallach, D., and Dobbelaere, D.A. (2002) Hijacking of host cell IKK signalosomes by the transforming parasite *Theileria*. *Science* **298:** 1033-1036.

Hinz, M., Krappmann, D., Eichten, A., Heder, A., Scheidereit, C., and Strauss, M. (1999) NF-kappaB function in growth control: regulation of cyclin D1 expression and G0/G1-to-S-phase transition. *Mol Cell Biol* **19:** 2690-2698.

Irvin,A.D. and Morrison,I.W. (1987) Immunopathology, immunology, and immunoprophylaxis of *Theileria* infections. In *Immune responses in parasitic infections: Immunology, immunopathology and immunoprophylaxis of Theileria infections*. Soulsby,E.J.L. (ed.) Baton Rouge, Florida: CRC Press Inc, pp. 223-274.

Ivanov, V., Stein, B., Baumann, I., Dobbelaere, D.A., Herrlich, P., and Williams, R.O. (1989) Infection with the intracellular protozoan parasite *Theileria parva* induces constitutively high levels of NF-kappa B in bovine T lymphocytes. *Mol Cell Biol* **9:** 4677-4686.

Kfoury, Y., Nasr, R., Favre-Bonvin, A., El Sabban, M., Renault, N., Giron, M.L., Setterblad, N., Hajj, H.E., Chiari, E., Mikati, A.G., Hermine, O., Saib, A., de The, H., Pique, C., and Bazarbachi, A. (2008) Ubiquitylated Tax targets and binds the IKK signalosome at the centrosome. *Oncogene* **27:** 1665-1676.

Kustermans, G., El Benna, J., Piette, J., and Legrand-Poels, S. (2005) Perturbation of actin dynamics induces NF-kappaB activation in myelomonocytic cells through an NADPH oxidase-dependent pathway. *Biochem J* **387:** 531-540.

LaCasse, E.C., Baird, S., Korneluk, R.G., and MacKenzie, A.E. (1998) The inhibitors of apoptosis (IAPs) and their emerging role in cancer. *Oncogene* **17:** 3247-3259.

Legrand-Poels, S., Kustermans, G., Bex, F., Kremmer, E., Kufer, T.A., and Piette, J. (2007) Modulation of Nod2-dependent NF-kappaB signaling by the actin cytoskeleton. *J Cell Sci* **120:** 1299-1310.

Loeb, K.R. and Haas, A.L. (1994) Conjugates of ubiquitin cross-reactive protein distribute in a cytoskeletal pattern. *Mol Cell Biol* **14:** 8408-8419.

Mortensen, K. and Larsson, L.I. (2003) Effects of cytochalasin D on the actin cytoskeleton: association of neoformed actin aggregates with proteins involved in signaling and endocytosis. *Cell Mol Life Sci* **60:** 1007-1012.

Nery, F.C., Zeng, J., Niland, B.P., Hewett, J., Farley, J., Irimia, D., Li, Y., Wiche, G., Sonnenberg, A., and Breakefield, X.O. (2008) TorsinA binds the KASH domain of nesprins and participates in linkage between nuclear envelope and cytoskeleton. *J Cell Sci* **121:** 3476-3486.

Oura, C.A., McKellar, S., Swan, D.G., Okan, E., and Shiels, B.R. (2006) Infection of bovine cells by the protozoan parasite *Theileria annulata* modulates expression of the ISGylation system. *Cell Microbiol* **8:** 276-288.

Palmer, G.H., Machado, J., Jr., Fernandez, P., Heussler, V., Perinat, T., and Dobbelaere, D.A. (1997) Parasite-mediated nuclear factor kappaB regulation in lymphoproliferation caused by *Theileria parva* infection. *Proc Natl Acad Sci U S A* **94:** 12527-12532.

Sager, H., Davis, W.C., Dobbelaere, D.A., and Jungi, T.W. (1997) Macrophage-parasite relationship in theileriosis. Reversible phenotypic and functional dedifferentiation of macrophages infected with *Theileria annulata*. *J Leukoc Biol* **61:** 459-468.

Schliwa, M. (1982) Action of cytochalasin D on cytoskeletal networks. *J Cell Biol* **92:** 79-91.

Schneider, I., Haller, D., Kullmann, B., Beyer, D., Ahmed, J.S., and Seitzer, U. (2007) Identification, molecular characterization and subcellular localization of a *Theileria annulata* parasite protein secreted into the host cell cytoplasm. *Parasitol Res* **101:** 1471-1482.

Schnittger, L., Katzer, F., Biermann, R., Shayan, P., Boguslawski, K., McKellar, S., Beyer, D., Shiels, B.R., and Ahmed, J.S. (2002) Characterization of a polymorphic *Theileria annulata* surface protein (TaSP) closely related to PIM of *Theileria parva*: implications for use in diagnostic tests and subunit vaccines. *Mol Biochem Parasitol* **120:** 247-256.

Shaw, M.K. (1997) The same but different: the biology of *Theileria* sporozoite entry into bovine cells. *Int J Parasitol* **27:** 457-474.

Shiels, B., Kinnaird, J., McKellar, S., Dickson, J., Miled, L.B., Melrose, R., Brown, D., and Tait, A. (1992) Disruption of synchrony between parasite growth and host cell division is a determinant of differentiation to the merozoite in *Theileria annulata*. *J Cell Sci* **101 (Pt 1):** 99-107.

Shiels, B., Swan, D., McKellar, S., Aslam, N., Dando, C., Fox, M., Ben Miled, L., and Kinnaird, J. (1998) Directing differentiation in *Theileria annulata*: old methods and new possibilities for control of apicomplexan parasites. *Int J Parasitol* **28:** 1659-1670.

Shiels, B.R., McKellar, S., Katzer, F., Lyons, K., Kinnaird, J., Ward, C., Wastling, J.M., and Swan, D. (2004) A *Theileria annulata* DNA binding protein localized to the host cell nucleus alters the phenotype of a bovine macrophage cell line. *Eukaryot Cell* **3:** 495-505.

Shiels, B.R., Smyth, A., Dickson, J., McKellar, S., Tetley, L., Fujisaki, K., Hutchinson, B., and Kinnaird, J.H. (1994) A stoichiometric model of stage differentiation in the protozoan parasite *Theileria annulata*. *Mol Cell Differ* **2:** 101-125.

Swan, D.G., Stadler, L., Okan, E., Hoffs, M., Katzer, F., Kinnaird, J., McKellar, S., and Shiels, B.R. (2003) TashHN, a *Theileria annulata* encoded protein transported to the host nucleus displays an association with attenuation of parasite differentiation. *Cell Microbiol* **5:** 947-956.

Swan, D.G., Stern, R., McKellar, S., Phillips, K., Oura, C.A., Karagenc, T.I., Stadler, L., and Shiels, B.R. (2001) Characterisation of a cluster of genes encoding *Theileria annulata* AT hook DNA-binding proteins and evidence for localisation to the host cell nucleus. *J Cell Sci* **114:** 2747-2754.

Weir, W., Ben Miled, L., Karagenc, T., Katzer, F., Darghouth, M., Shiels, B., and Tait, A. (2007) Genetic exchange and sub-structuring in *Theileria annulata* populations. *Mol Biochem Parasitol* **154:** 170-180.

Figure 1

A

Marker	D7 (bp)	D7 B12 (bp)
TS5	282	282
TS6	389	389
TS8	305	305
TS9	364	364
TS12	267	267
TS15	284	284
TS16	353	353
TS20	273	273
TS25	280	280
TS31	313	313

B

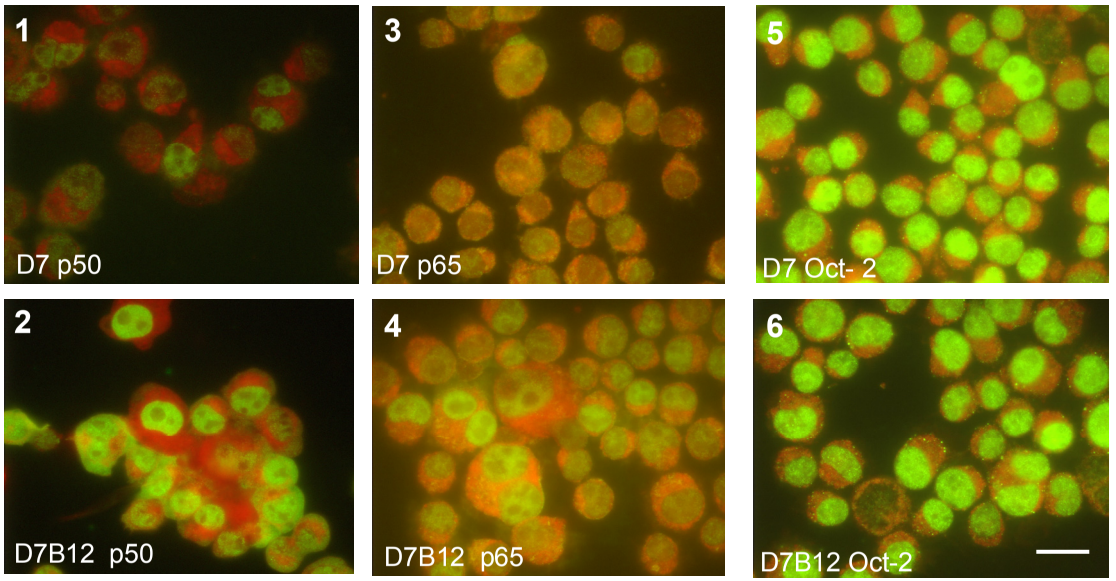

C

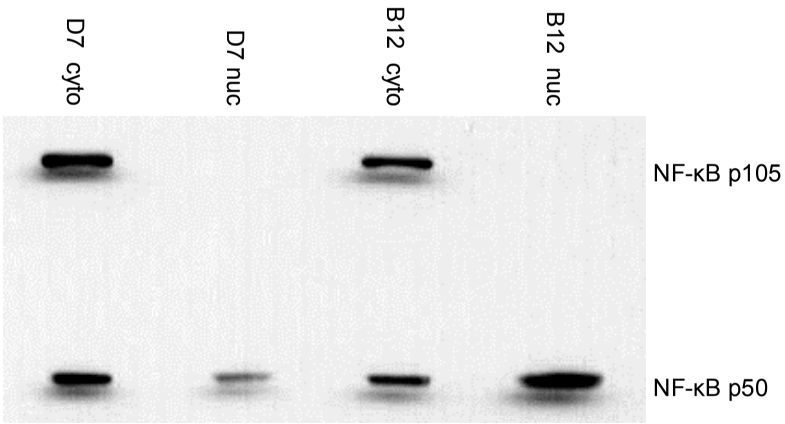

D

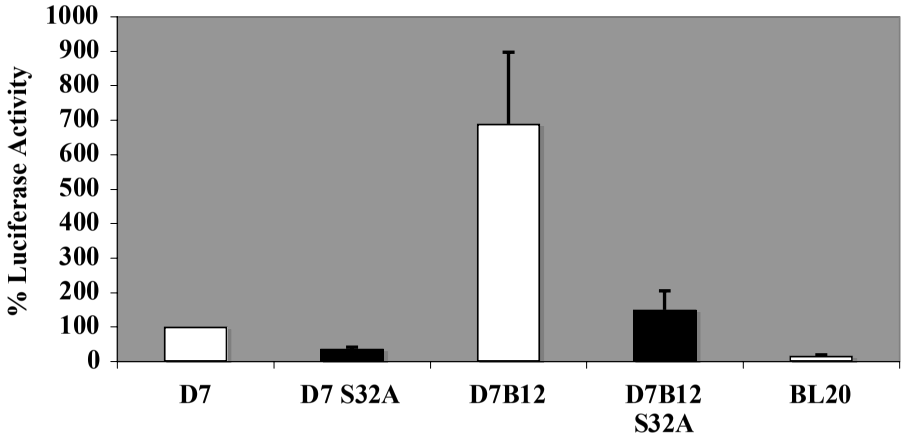

Figure 2

A

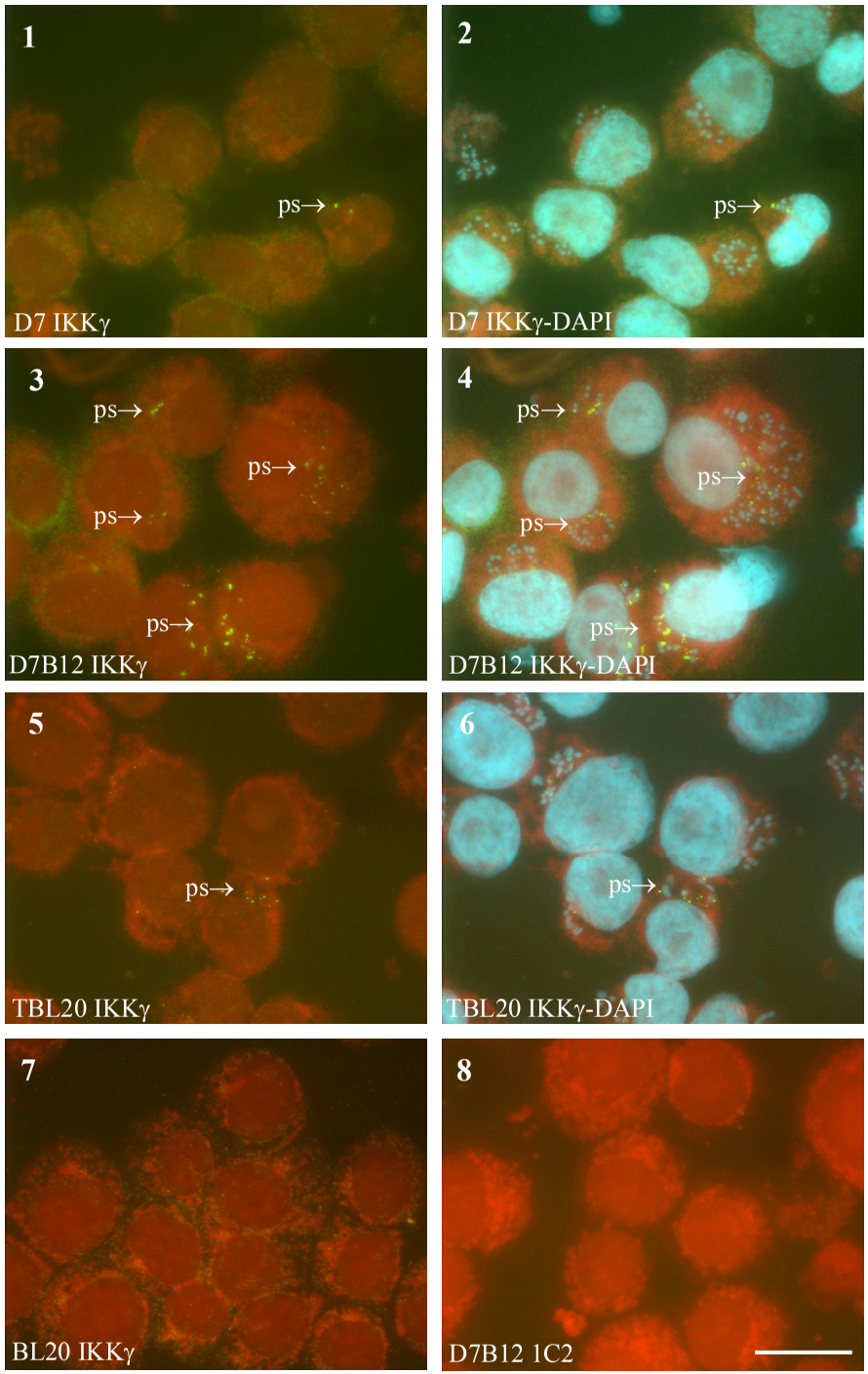
1
ps→
D7 IKKγ
2
ps→
D7 IKKγ-DAPI
3
ps→
ps→
ps→
ps→
D7B12 IKKγ
4
ps→
ps→
ps→
ps→
D7B12 IKKγ-DAPI
5
ps→
TBL20 IKKγ
6
ps→
TBL20 IKKγ-DAPI
7
BL20 IKKγ
8
D7B12 1C2

B

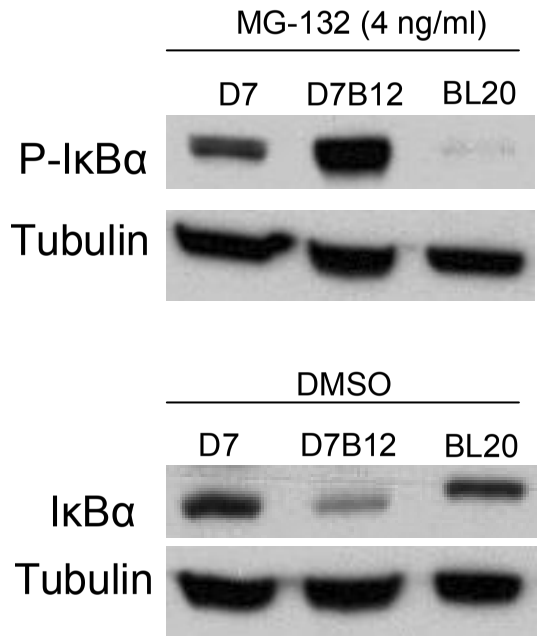
MG-132 (4 ng/ml)
D7
D7B12
BL20
P-IκBα
Tubulin
DMSO
D7
D7B12
BL20
IκBα
Tubulin

Figure 3

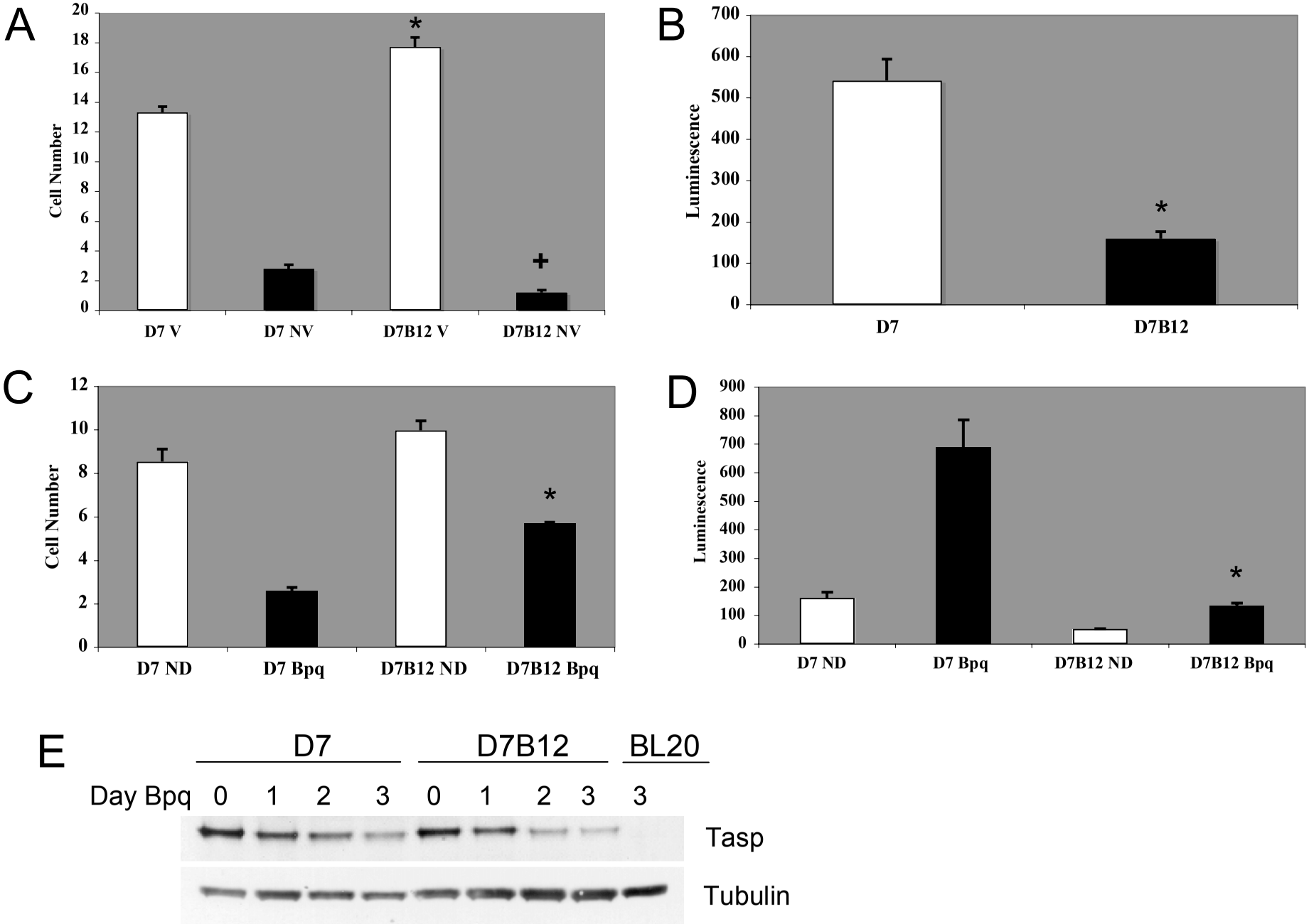
A
Cell Number
20
18
16
14
12
10
8
6
4
2
0
*
+
D7 V
D7 NV
D7B12 V
D7B12 NV
B
Luminescence
700
600
500
400
300
200
100
0
*
D7
D7B12
C
Cell Number
12
10
8
6
4
2
0
*
D7 ND
D7 Bpq
D7B12 ND
D7B12 Bpq
D
Luminescence
900
800
700
600
500
400
300
200
100
0
*
D7 ND
D7 Bpq
D7B12 ND
D7B12 Bpq
E
D7
D7B12
BL20
Day Bpq 0 1 2 3 0 1 2 3 3
Tasp
Tubulin

Figure 4

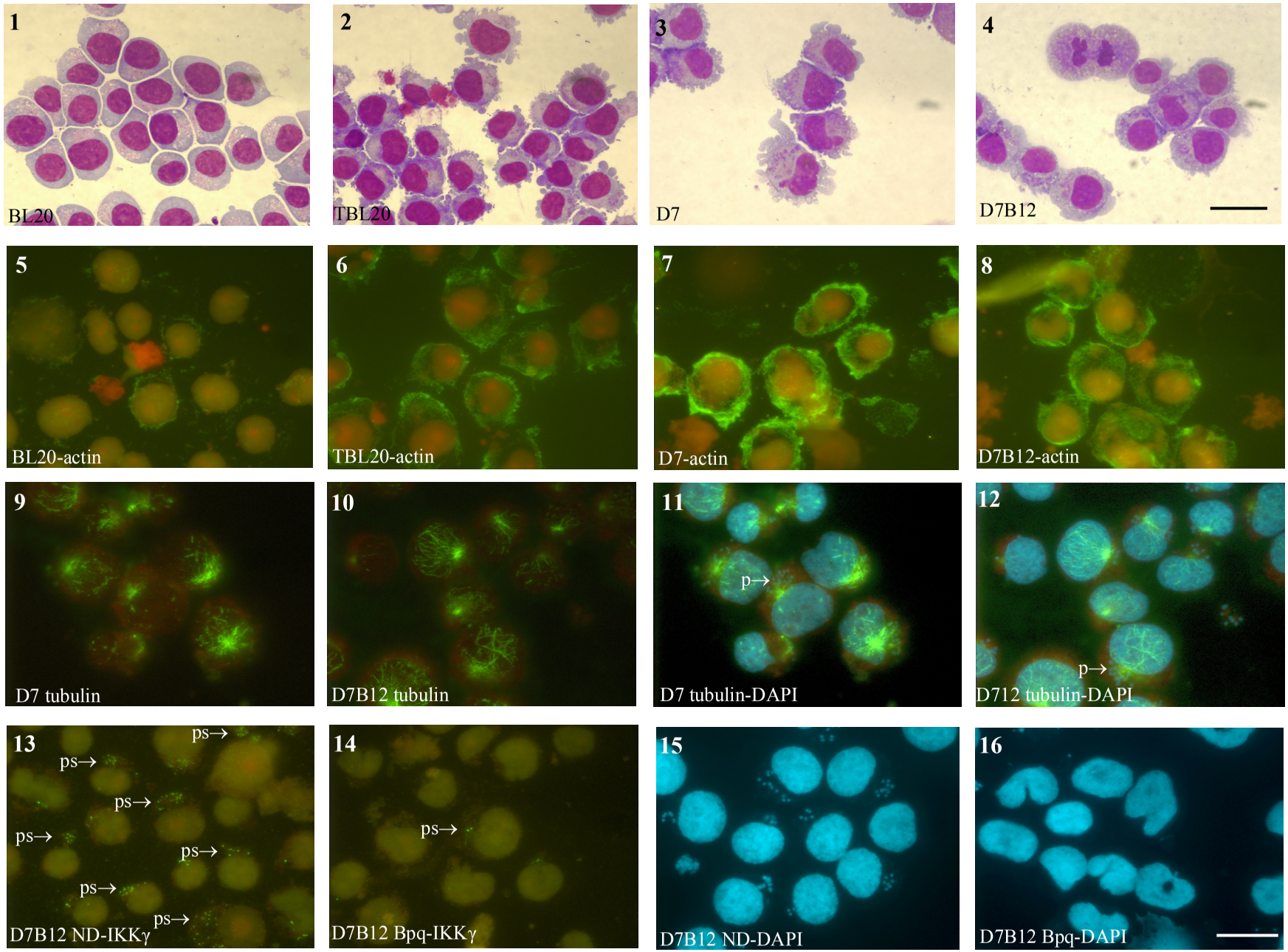
1
BL20
2
TBL20
3
D7
4
D7B12
5
BL20-actin
6
TBL20-actin
7
D7-actin
8
D7B12-actin
9
D7 tubulin
10
D7B12 tubulin
11
p→
D7 tubulin-DAPI
12
p→
D712 tubulin-DAPI
13
ps→
ps→
ps→
ps→
ps→
ps→
ps→
D7B12 ND-IKKγ
14
ps→
D7B12 Bpq-IKKγ
15
D7B12 ND-DAPI
16
D7B12 Bpq-DAPI

Figure 5

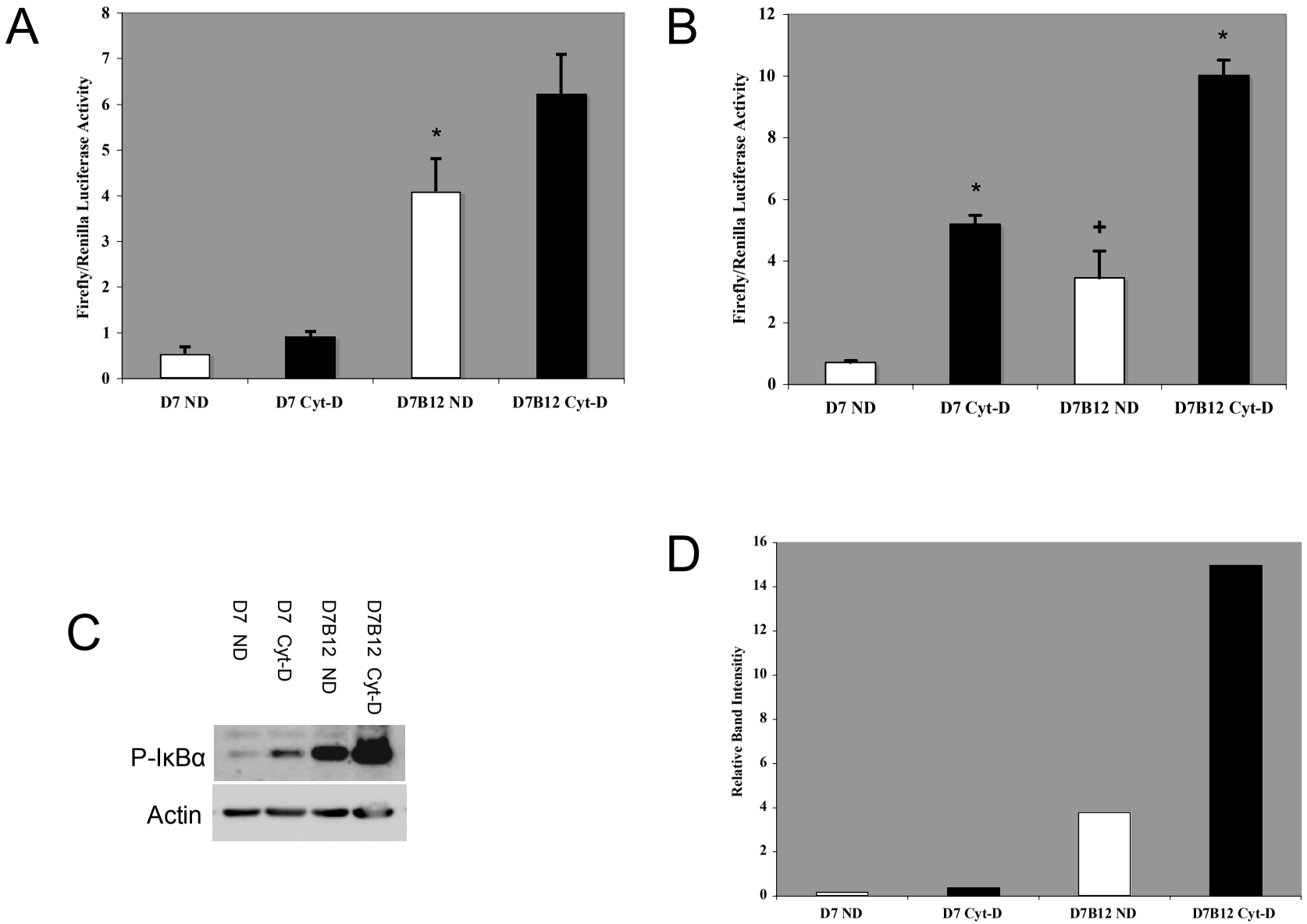
A
Firefly/Renilla Luciferase Activity
0
1
2
3
4
5
6
7
8
*
D7 ND
D7 Cyt-D
D7B12 ND
D7B12 Cyt-D
B
Firefly/Renilla Luciferase Activity
0
2
4
6
8
10
12
*
*
+
D7 ND
D7 Cyt-D
D7B12 ND
D7B12 Cyt-D
C
D7 ND
D7 Cyt-D
D7B12 ND
D7B12 Cyt-D
P-IκBα
Actin
D
Relative Band Intensitiy
0
2
4
6
8
10
12
14
16
D7 ND
D7 Cyt-D
D7B12 ND
D7B12 Cyt-D

Figure 6

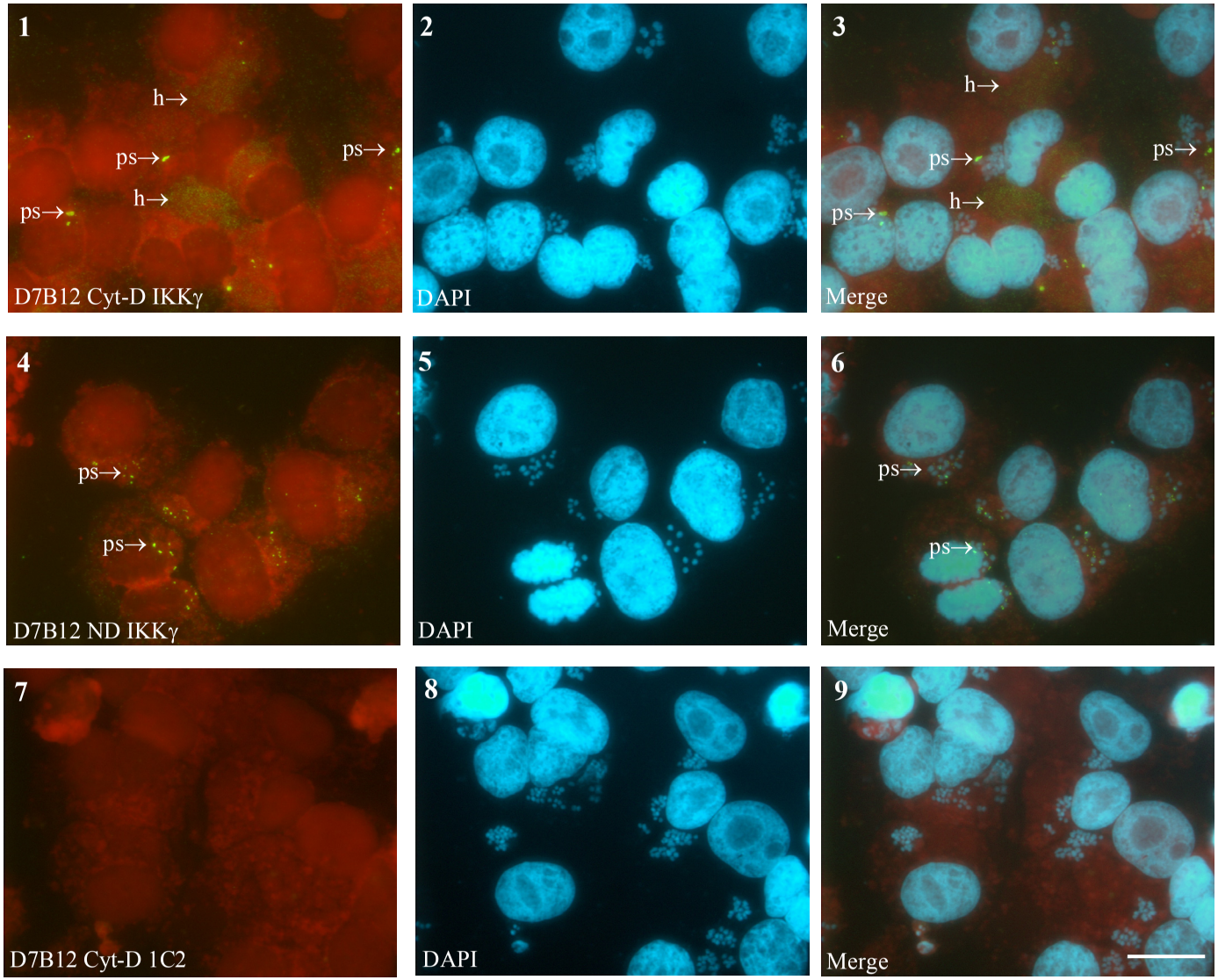
1
h→
ps→
ps→
h→
ps→
D7B12 Cyt-D IKKγ
2
DAPI
3
h→
ps→
ps→
ps→
h→
Merge
4
ps→
ps→
D7B12 ND IKKγ
5
DAPI
6
ps→
ps→
Merge
7
D7B12 Cyt-D 1C2
8
DAPI
9
Merge

Figure 7

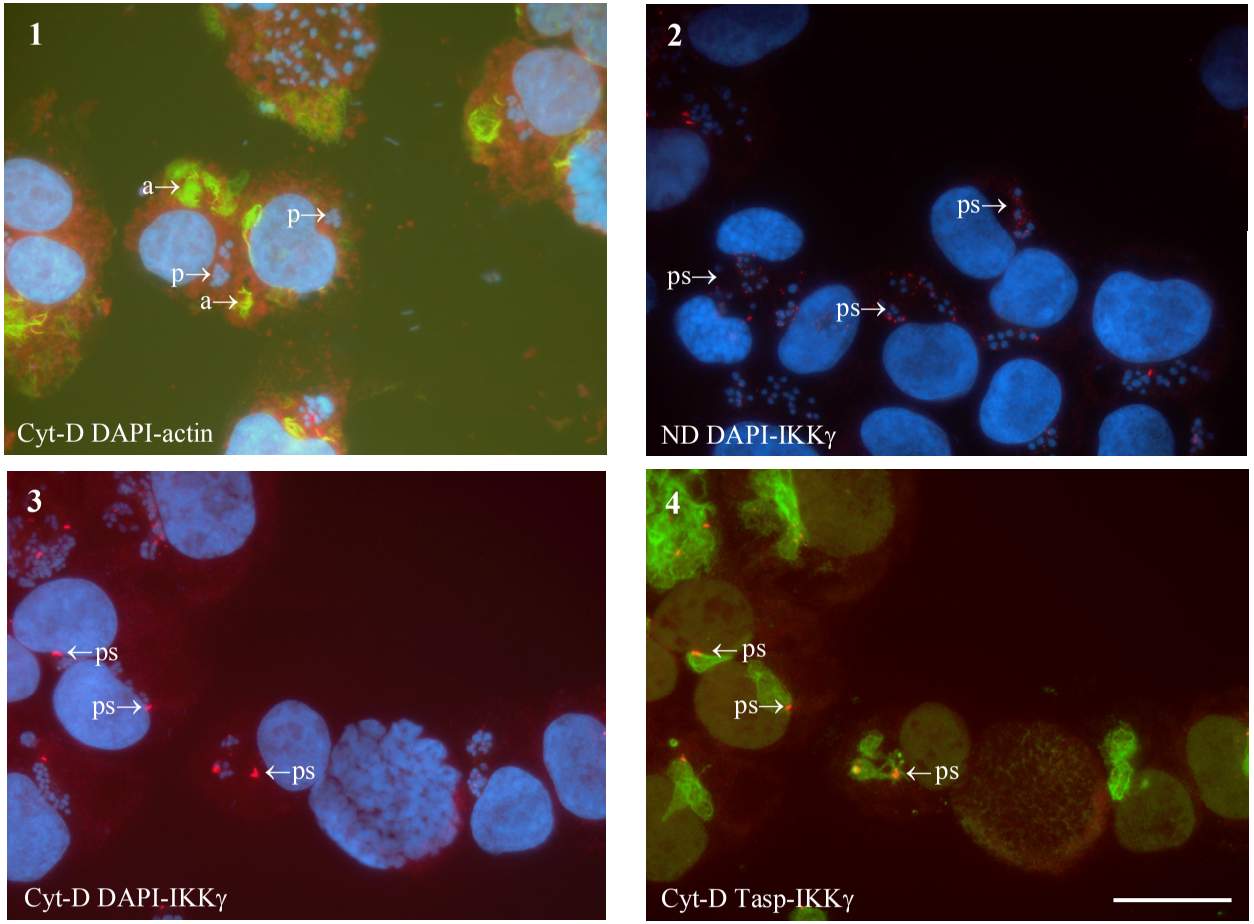
1
a→
p→
p→
a→
Cyt-D DAPI-actin
2
ps→
ps→
ps→
ND DAPI-IKKγ
3
←ps
ps→
←ps
Cyt-D DAPI-IKKγ
4
←ps
ps→
←ps
Cyt-D Tasp-IKKγ

Figure 8

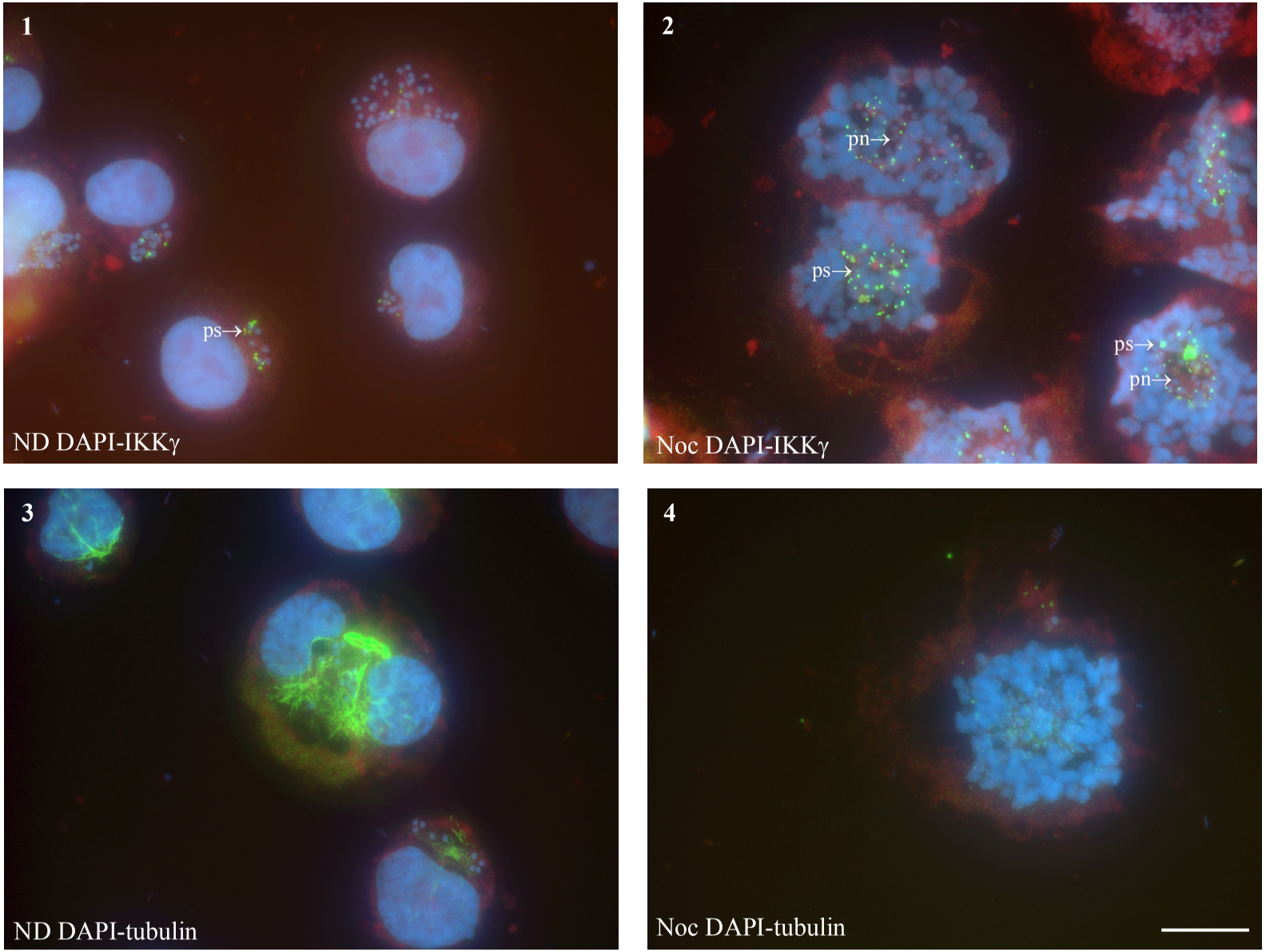
1
ps→
ND DAPI-IKKγ
2
pn→
ps→
ps→
pn→
Noc DAPI-IKKγ
3
ND DAPI-tubulin
4
Noc DAPI-tubulin

Supplementary Data Figure 1

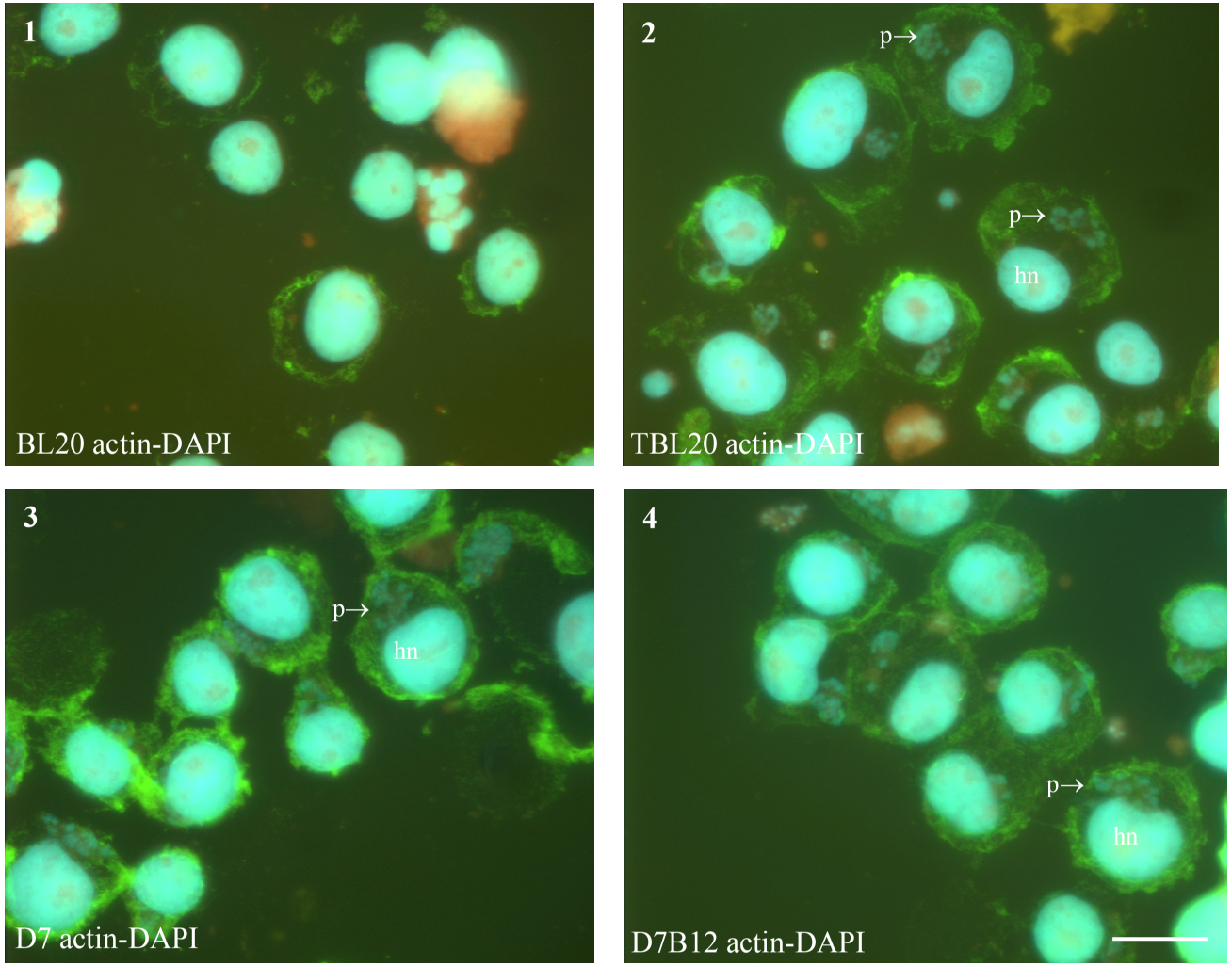

Supplementary Data Figure 2

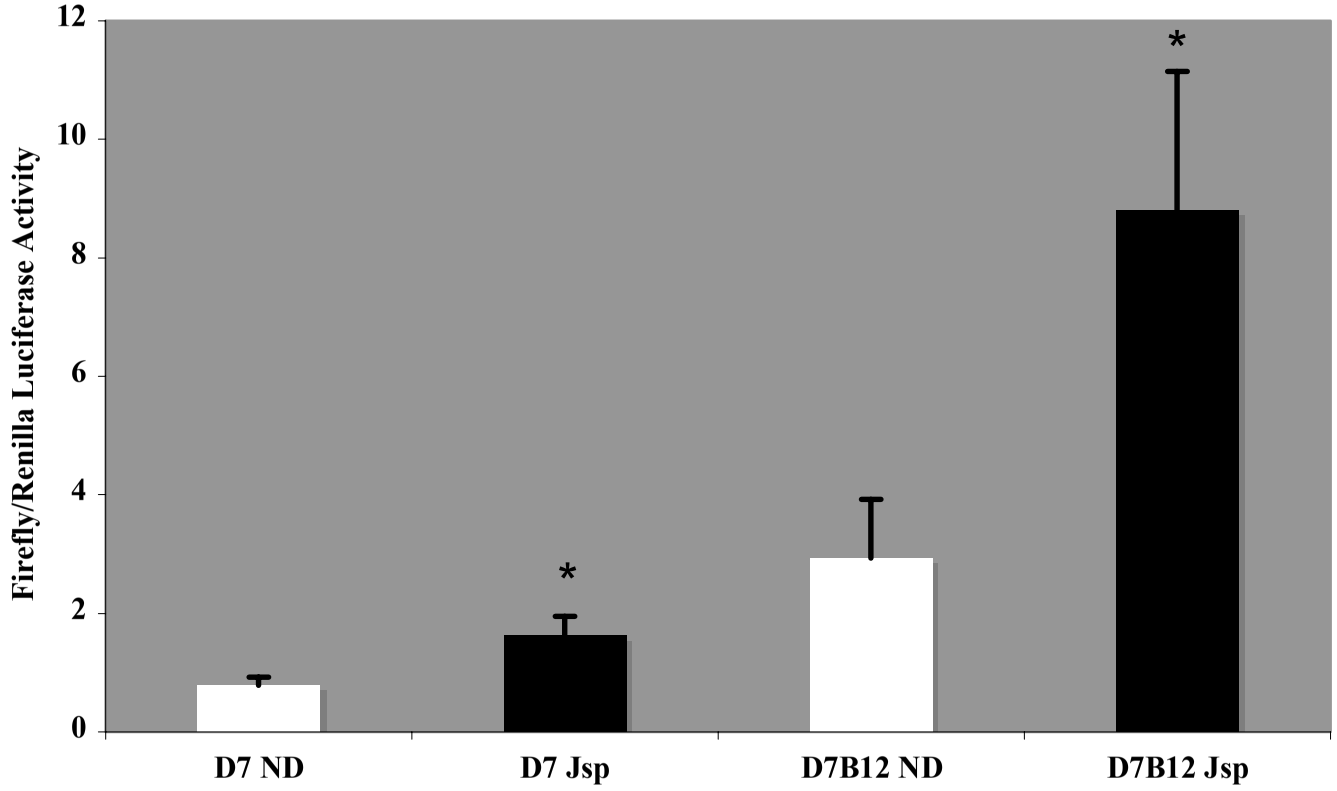

Supplementary Data Figure 3

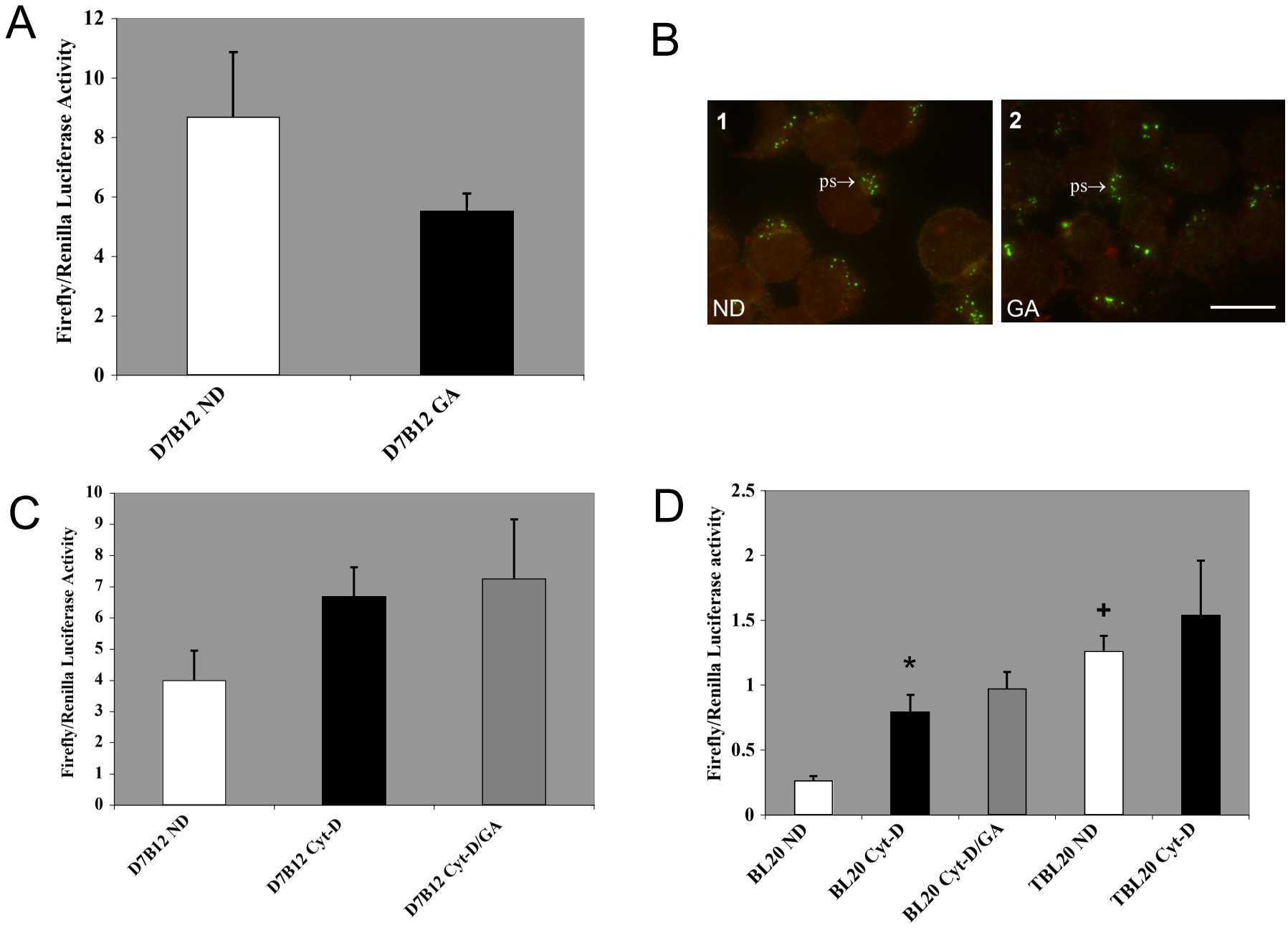

Supplementary Data Figure 4

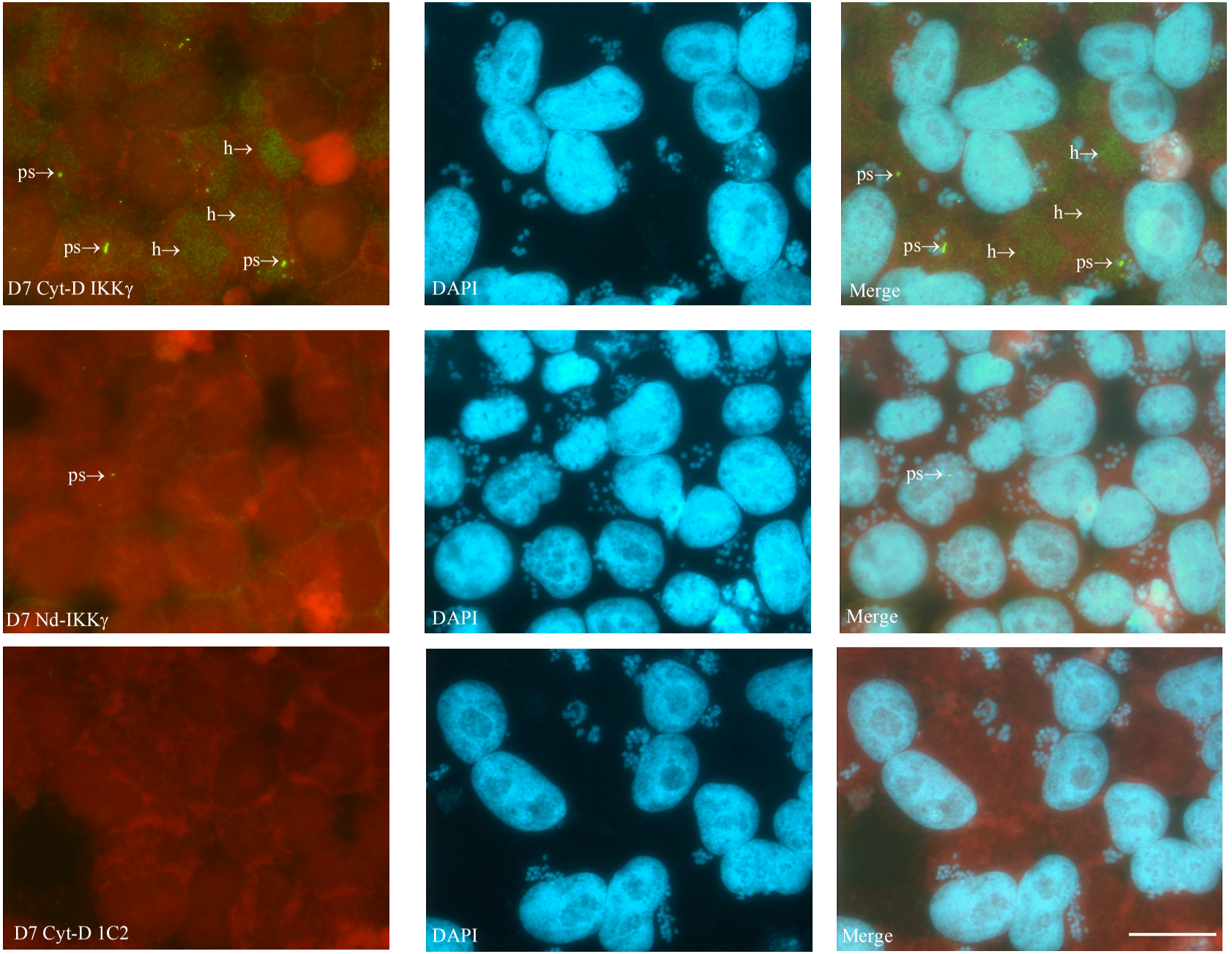

Supplementary Data Figure 5

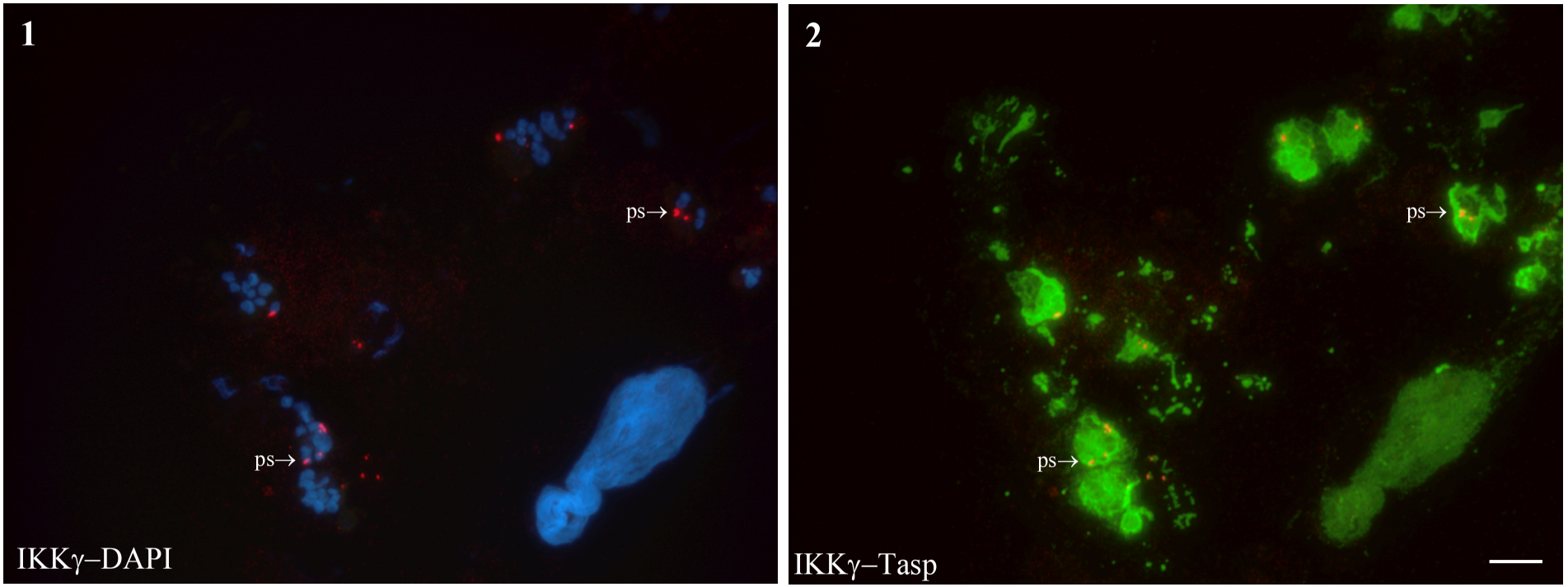

Supplementary Data Figure 6